Master's thesis

NTNU
Norwegian University of Science and Technology
Faculty of Medicine and Health Sciences
Department of Clinical and Molecular Medicine

Ahmed Sabbir

# Deciphering role of succinate in metabolic rewiring of innate immunity

Master's thesis in Molecular Medicine
Supervisor: Richard Kumaran Kandasamy
Co-supervisor: Yashwanth Subbannayya
June 2021

NTNU
Kunnskap for en bedre verden

Ahmed Sabbir

# Deciphering role of succinate in metabolic rewiring of innate immunity

Master's thesis in Molecular Medicine
Supervisor: Richard Kumaran Kandasamy
Co-supervisor: Yashwanth Subbannayya
June 2021

Norwegian University of Science and Technology
Faculty of Medicine and Health Sciences
Department of Clinical and Molecular Medicine

NTNU
Norwegian University of
Science and Technology

## ABSTRACT

Succinate is the anionic form of succinic acid, which is produced during adenosine triphosphate (ATP) synthesis via the tricarboxylic acid (TCA) cycle. In a biological system, succinate can be found in two forms. One is diethyl succinate which is cell-permeable, while the other form, disodium succinate, is cell non-permeable. Succinate has been found to be associated with inflammation through activation of the Toll-like receptor 4 (TLR4). However, succinate has also been found to induce both proinflammatory and anti-inflammatory cytokines. The aim of this project was to study how succinate affects the TLR4 inflammatory signaling. Lipopolysaccharide (LPS) is a well-established inflammatory cytokine inducer and is a ligand for TLR4. In this project, the experimental settings investigated how succinate affects the TLR4 signaling in the THP-1 cell line. For the experiments, phorbol-12-myristate-13-acetate (PMA) was used to differentiate THP-1 monocytes into macrophages, which were then stimulated with the four conditions: untreated control, LPS, disodium succinate, and a combination of LPS and disodium succinate. Western blots were performed to figure out which TLR4 signaling mediators were activated. RT-qPCR was conducted to investigate how succinate affects inflammatory cytokine release. Western blot results suggested that both LPS and disodium succinate activated the MyD88-dependent TLR4 signaling pathway strongly comparing to the MyD88-independent pathway. Furthermore, disodium succinate has been found to dampen; probably regulate LPS induced cytokine production. *18S* and *GAPDH* were selected as endogenous controls for analyzing the mRNA expression of *TNF-α*, *IL-1β*, *MMP9*, and *TGF-β1* inflammatory cytokines. The data suggest that both LPS and disodium succinate induced inflammatory cytokine release. Disodium succinate reduced LPS-induced mRNA expression of *TNF-α* and *IL-1β*, whereas no significant changes were observed with respect to *MMP9* and *TGF-β1* levels. To summarize, disodium succinate can strongly activate TLR4 signaling through MyD88-dependent, same as LPS. Both LPS and disodium succinate can induce inflammatory cytokine production. Furthermore, disodium succinate can probably regulate LPS induced inflammatory cytokines through disodium succinate-LPS crosstalk. However, the inflammation regulatory mechanism of succinate requires further investigation.

## ACKNOWLEDGMENTS

I would first like to thank my supervisor Dr. Richard Kumaran Kandasamy, for giving me a lot of freedom to explore topics I am interested in and for always providing such invaluable support and assistance. I would also like to thank my co-supervisor Yashwanth Subbannayya, for teaching me the experimental methods in such a short period of time during the COVID-19 pandemic and helping with the manuscript. I also wish to express my thanks to Claire Louet for teaching me a lot about PCR and helping with my data analysis.

I would also like to thank everyone in the laboratory for always being willing to lend a helping hand, be it with experiments or on how to survive Trondheim winters.

Finally, I must express my very profound gratitude to my family and friends for providing me with unfailing support and continuous encouragement throughout my years of study and through the process of researching and writing this thesis. This accomplishment would not have been possible without them. Thank you.

# TABLE OF CONTENT

**Abstract** ..... **v**

**Acknowledgments** ..... **vi**

**Table of content** ..... **vii**

**List of figures** ..... **x**

**List of tables** ..... **x**

**Abbreviations** ..... **xi**

**1. Introduction** ..... **1**

1.1. Immune system ..... 1

1.2. Innate immunity ..... 2

1.3. Pattern Recognition Receptors (PRRs) ..... 3

1.4. Inflammasome ..... 4

1.5. Toll-Like Receptors (TLRs) ..... 4

1.5.1. TLR family ..... 7

1.5.2. TLR4 ..... 8

1.5.3. TLR4 signaling ..... 8

1.5.4. MyD88-independent/TRIF-dependent pathway ..... 9

1.5.5. MyD88-dependent pathway ..... 10

1.5.6. Lipopolysaccharide (LPS) ..... 11

1.5.7. Mimicking TLR4 signaling in macrophages with lipopolysaccharide (LPS) ..... 11

1.6. Monocytes and macrophages ..... 12

1.6.1 Polarization of macrophages ..... 13

1.7. THP-1 cell line as monocyte and macrophage response model ..... 15

1.8. Immunometabolism ..... 16

1.9. Succinate ..... 16

1.9.1. Succinate in TCA cycle ..... 16
1.9.2. Succinate accumulation through TLR4 activation ..... 17
1.9.3. Succinate stabilizes HIF-1α allowing inflammatory cytokine secretion via mitochondrial ROS generation ..... 17
1.9.4. Succinate induces “Warburg effect” in hypoxic conditions ..... 18
1.9.5. Proinflammatory and anti-inflammatory activity of succinate ..... 18
**2. Aim ..... 20**
**3. Materials and methods ..... 21**
3.1. THP-1 Cell culture ..... 21
3.1.1. Cell culture condition ..... 21
3.1.1.1. Equipment and reagents ..... 21
3.1.1.2. Procedure ..... 21
3.1.2. Cell counting ..... 22
3.2. Cell differentiation ..... 22
3.2.1. Principle ..... 22
3.2.2. Procedure ..... 22
3.3. Experimental conditions ..... 23
3.3.1. Cell stimulation with experimental conditions ..... 23
3.4. Protein extraction ..... 24
3.4.1. Reagents and equipment ..... 24
3.4.2. Principle ..... 24
3.4.3. Procedure ..... 24
3.5. Total protein estimation ..... 25
3.5.1. Reagents and equipment ..... 25
3.5.2. Principle ..... 25

3.5.2. Procedure ..... 26
3.6. Western blot ..... 26
3.6.1. Reagents ..... 26
3.6.2. Principle ..... 27
3.6.3. Procedure ..... 30
3.7. Reverse-transcription polymerase chain reaction (RT-qPCR) ..... 31
3.7.1. Reagents ..... 31
3.7.2. Principles ..... 32
3.7.2.1. RNA extraction, purification, and quantification ..... 32
3.7.2.2. Reverse-transcription (RT) ..... 33
3.7.2.3. RT-qPCR ..... 33
3.7.3. RT-qPCR Procedure ..... 35
**4. Results ..... 37**
4.1. Succinate strongly induces TLR4 signaling through MyD88-dependent pathway ..... 37
4.2. Succinate-LPS crosstalk probably regulates LPS-induced MyD88-dependent TLR4 signaling. ..... 39
4.3. Primer specificity analysis of RT-qPCR. ..... 40
4.4. *18S* and *GAPDH* genes serve as endogenous controls for THP-1 cells perturbed with succinate ..... 43
4.5. mRNA expression of TLR4 induced cytokines ..... 45
**5. Discussion ..... 46**
**6. Limitations ..... 50**
**7. Conclusion ..... 51**
**8. Future plans ..... 51**
**9. References ..... 52**
**Appendix ..... 59**

## LIST OF FIGURES

Figure 1.1: Cellular components of the innate and adaptive immune response ……. 2
Figure 1.2: A representative structure of membrane-bound TLR ....…….. 5
Figure 1.3: A schematic representation of human TLR signaling pathways ...…….. 6
Figure 1.4: Overview of LPS induced TLR4 signaling pathways ...…….. 8
Figure 1.5: LPS induced MyD88-independent TLR4 signaling pathway ...…….. 9
Figure 1.6: LPS induced MyD88-dependent TLR4 signaling pathway ……... 10
Figure 1.7: Inducing factors and functional properties of different polarized macrophages ... 14
Figure 4.1: Succinate-LPS crosstalk dampens TLR4 signaling through both MyD88-dependent pathways ……... 38
Figure 4.2: RT-qPCR melting curve analysis of target genes …….. 41
Figure 4.3: Gel electrophoresis of PCR products ……..…….. 42
Figure 4.4: *18S*, *ACTB*, *GAPDH* and *TBP* gene amplification in average number of RT-qPCR cycle …….. 44
Figure 4.5: mRNA expression level of *TNF-α*, *IL-1β*, *MMP9* and *TGF-β1* inflammatory cytokines ……..…….. 45

## LIST OF TABLES

Table 1.1: Functions of innate immune cells ……....3
Table 1.2: Overview of human TLRs, highlighting their known ligands, localization, adaptor proteins and end products used to initiate signaling pathways including, the commonly induced cytokines ……..…..……...7
Table 1.3: Macrophage receptors implicated in PAMPs recognition ….……....13
Table 3.1: Primary and secondary antibodies used in western blot ……27
Table 4.1: Report of $C_T$ value mean of target genes from RT-qPCR ..……43

## ABBREVIATIONS

| | |
|---|---|
| AIM2 | Absent in melanoma 2 |
| AP-1 | Adaptor protein- 1 |
| APC | Antigen-presenting cell |
| ATCC | American Type Culture Collection |
| ATP | Adenosine triphosphate |
| BMDM | Bone marrow-derived macrophages |
| BSA | Bovine serum albumin |
| CD14 | Cluster of differentiation 14 |
| CD36 | Cluster of differentiation 36 |
| CR3 | Complement receptor 3 |
| CCR2 | C-C chemokine receptor type 2 |
| CLR | C-type lectin receptor |
| Coq | Co-enzyme Q |
| CXCL9 | Chemokine (C-X-C motif) ligand 9 |
| DAMP | Damage associated molecular pattern |
| DC | Dendritic cell |
| DTT | Dithiothreitol |
| ETC | Electron transport chain |
| FBS | Fetal Bovine Serum |
| FCS | Fetal Calf serum |
| GPR91 | G-protein coupled receptor 91 |
| HIF-1α | Hypoxia Inducing Factor- 1α |
| HRP | Horse Radish Peroxidase |
| IFI 16 | Interferon-inducible protein 16 |
| IFN | Interferon |
| IL | Interleukin |
| IRAK | IL-1 Receptor-Associated Kinases |
| IRF | Interferon regulatory factors |
| LBP | LPS binding protein |
| LDH | Lactate dehydrogenase |
| LDS | Lithium dodecyl sulfate |
| LPS | Lipopolysaccharides |
| LRR | Leucine-rich repeat |
| iNOS | Inducible nitric oxide synthase |
| M1 | Classically activated macrophages |
| M2 | Alternatively activated macrophages |
| MAL | Myeloid adapter-like protein |
| MAPK | Mitogen-activated protein kinase |
| MD-2 | Myeloid Differentiation Factor-2 |

| | |
|---|---|
| MHC-II | Major histocompatibility complex class II |
| MKP-1 | MAPK phosphatase-1 |
| MOPS | 3-(N-morpholino) propane sulfonic acid |
| Myd88 | Myeloid differentiation factor 88 |
| NEMO | NF-κB essential modulator |
| NF-κB | Nuclear factor kappa B |
| NK cell | Natural killer cell |
| Nod | Nucleotide-binding oligomerization domain |
| NLR | Nod and leucine-rich repeat-containing receptor |
| NLRP3 | NLR protein 3 |
| PAMP | Pathogen associated molecular pattern |
| PBS | Dulbecco's Phosphate Buffered Saline |
| PHD | Prolyl hydroxylases |
| PMA | Phorbol-12-myristate-13-acetate |
| PMN cell | Polymorphonuclear cell |
| PRR | Pattern recognition receptor |
| PVDF | Polyvinylidene difluoride |
| RIG-I | Retinoic acid-inducible gene-I-like receptor |
| RIP1 | Receptor-interacting serine/threonine-protein 1 |
| RT-qPCR | Reverse transcription quantitative polymerase chain reaction |
| SDH | Succinyl dehydrogenase |
| SDS | Sodium dodecyl sulfate |
| SR-A | Scavenger receptor A |
| STAT | Signal Transducer and Activator of Transcription |
| SUCNR1 | Succinate receptor 1 |
| TABs | (TAK1)-binding proteins |
| TAK1 | (TGF-β1)-activated kinase 1 |
| TBK1 | TANK-binding kinase 1 |
| TCA | Tricarboxylic acid |
| TEAB | Triethylammonium bicarbonate |
| Th2 | Type II helper T cell |
| TIR | Toll interleukin-1 receptor |
| TIRAP | TIR Domain-Containing Adaptor Protein |
| TGF-β | Transforming growth factor β |
| TLR | Toll-like receptor |
| TNF-α | Tumor necrosis factor- α |
| TRAF | Tumor necrosis factor receptor (TNFR)-associated factor |
| TRAM | TRIF-related adapter molecule |
| TRIF | TIR-domain containing adaptor inducing protein inducing IFN-β |
| Vd3 | 1α, 25-dihydroxyvitamin D3 |

# 1. INTRODUCTION

## 1.1. Immune system

The human immune system is an intertwined defensive mechanism against the invasion of foreign particles such as pathogens and toxins. The immune system is known to respond to both endogenous and exogenous danger signals affecting the overall homeostasis of the body[1]. In case the immune system is compromised due to immunodeficiencies (increased susceptibility towards infections), autoimmunity disorder (the immune system itself becomes a threat for the body), etc., the system functions differently[2,3]. Both components of the cellular immune system, namely, innate, and adaptive immune systems, act closely together to achieve such defensive maneuvers. The innate immune system acts as the first wall of defense and responds quickly but with limited potency. The system utilizes barriers, both physical and chemical, alongside the complement systems, monocytes, macrophages, granulocytes, dendritic cells (DCs), and natural killer (NK) cells. Soluble factors like complement proteins are also a part of the innate immune system. In case the innate response fails to eliminate the pathogen, the adaptive immune response initiates. Unlike the innate response, the adaptive response is very potent but requires more time to act. Utilizing both humoral responses mediated by B-cell and antibodies and cell-mediated responses mediated by cytotoxic and helper T cells, adaptive immune response recognizes antigens with high specificity. Although this process can take from several days to weeks to generate such specific responses, the adaptive immune system can generate immunological memory, which upon re-exposure to a similar pathogen can provide fast and vigorous immune response[4]. As previously mentioned, in addition to cellular immunity, the humoral immune response is vital for the effective functioning of the overall immune system. While the cellular immune system utilizes different cytokines to nullify pathogenic attacks, the humoral immune response is initiated by the secretion of different antibodies produced by B cells in association with T cells[5,6]. The innate and adaptive immune systems are interconnected and function in collaboration with each other to protect the body from foreign invaders[7,8].

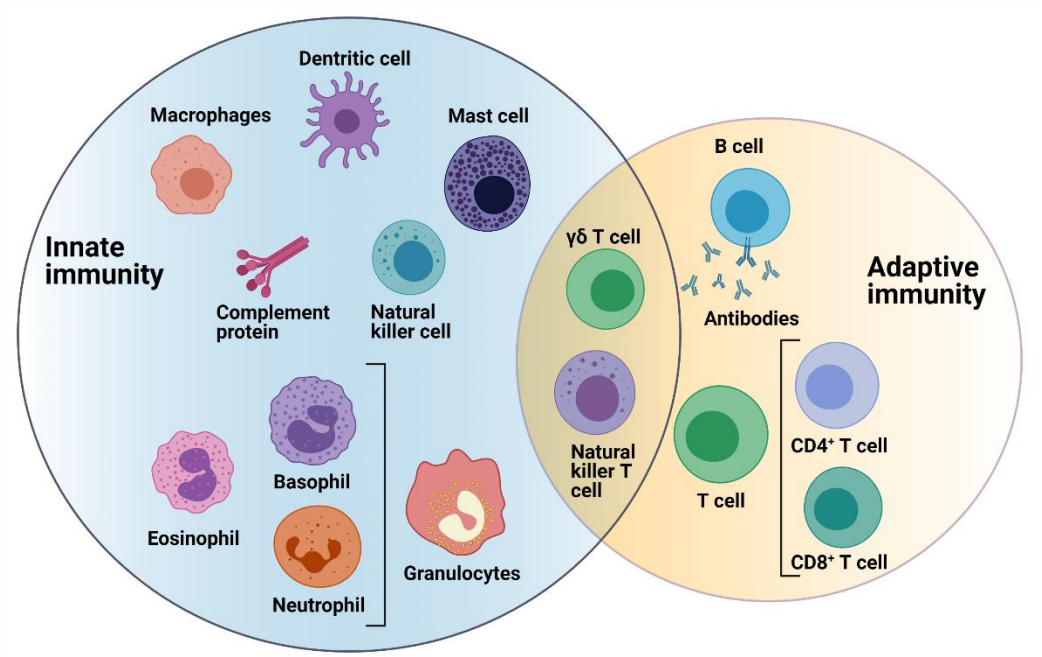


**Figure 1.1: Cellular components of the innate and adaptive immune response.**

The rapid innate immune response is generated through soluble factors, such as complement proteins, and a wide range of cellular components, including macrophages, dendritic cells, mast cells, NK cells, and granulocytes (basophils, eosinophils, and neutrophils). The slowly developed adaptive immune response is mediated through antibodies, B cells, and CD4+ and CD8+ T lymphocytes with higher antigenic specificity and memory. NK T cells and γδ T cells are cytotoxic lymphocytes functioning at the intersection of the innate and adaptive immune response. The figure was modified from "The innate and adaptive immune response" by Dranoff, G *et al.*[8]).

## 1.2. Innate immunity

As illustrated in figure 1.1, a wide range of cellular components actively participate in generating the rapid innate immune response[8]. In addition, epithelial barriers, such as the skin and lining cells in the gastrointestinal tract, lungs, and urinary tract, are also part of the system[9]. Together, the barriers and cells can provide immediate defense against infection within 4-96 hrs. The immediate immune response is initiated by general molecular or pattern recognition mechanisms, which can detect invading foreign pathogens such as bacteria, fungi, or viruses. Although this response is for short-term immunity only, it can, however, lead to long-lasting pathogen-specific response activation of the adaptive immune system[10]. Utilizing a wide range of receptors encoded by different genes, the adaptive immune cells can provide specific immunity to the host[11].

Some of the major roles of the innate immune system are (i) activation of Pattern Recognition Receptors (PRRs) to recognize foreign pathogens, (ii) elimination of pathogens by modulating cell proliferation, (iii) production of proinflammatory cytokines to recruit effector cells at the site of infection and anti-inflammatory cytokines when the infectious condition is ameliorated and (iv) phagocytosis to engulf and digest pathogens[12]. The core functions of different innate immune cells are listed in **Table 1.1**.

**Table 1.1: Functions of innate immune cells.**

| Innate immune cells | Functions |
|---|---|
| Neutrophils | Engulfing of invading pathogens and inflammation |
| Basophils | Secretion of histamine and inflammation |
| Eosinophils | Structural integrity disruption of worms and hypersensitive reactions |
| Monocytes | Engulfing of invading pathogens and differentiation into macrophages |
| Macrophages | Engulfing invading pathogens and activation of T cells |
| Mast cells | Initiation of inflammatory response |
| Natural killer cells | Antibody signal-dependent cell rupture |
| Dendritic cells | Antigen presentation to T cells |

### 1.3. Pattern Recognition Receptors (PRRs)

The initial response to an invading organism is set in motion by phagocytes such as neutrophils, macrophages, and DCs. These cells identify pathogens over themselves via PRRs. PRRs recognize pathogen-associated molecular patterns (PAMPs), and the following response depends on the origin of PAMPs, and which PRRs have been activated. Based on the localization of PRRs, they can be of different types. Membrane-bound PRRs can be Toll-like receptors (TLRs), and C-type lectin receptors (CLR), while cytosolic PRRs can be retinoic acid-inducible gene-I-like receptors (RIG-I), and nucleotide-binding and oligomerization domain (NOD)-like receptors (NLRs) which include NODs and NLR proteins (NLRPs). PRRs can also be activated by endogenous stress or damage signals, damage-associated molecular patterns (DAMPs).

### 1.4. Inflammasome

Inflammasomes are cytosolic multiprotein oligomers responsible for the activation of inflammatory innate immune responses. They consist of (i) NLRs and (ii) absent in melanoma 2 (AIM2)-like receptors (ALRs)[13]. Upon activation and assembly, inflammasomes promote proteolytic cleavage, maturation, and secretion of proinflammatory cytokines (i.e., IL-1β, IL-18)[13]. They are also responsible for the cleavage of Gasdermin-D by fragmentation of the N-terminal and plasma membrane pore formation[14]. The cleaved Gasdermin-D induces proinflammatory cytokines, which are secreted into the extracellular space through the pores[13].

When an infection occurs, the innate immune response immediately activates the PRRs[15]. One of the most extensively studied PRRs, TLRs, specifically TLR4, has been found to promote the inflammatory cascade of NLR protein-3 (NLRP3)[16]. Further investigation concreted the association between NLRP3 inflammasome and TLR4/MyD88/NF-κB signaling pathway[17]. Zhang and colleagues utilized Lipopolysaccharide (LPS) to induce TLR4/MyD88/NF-κB signaling pathway, which promoted NLRP3 inflammasome activation resulting in aggravated inflammatory response[18]. Activated TLR4/MyD88/NF-κB signaling pathway also activates NF-κB, which regulates cytokine production and NLRP3 inflammasome[17,19]. This finding was further investigated where the same TLR4/MyD88/NF-κB signaling pathway was inhibited, which led to reduced LPS-induced inflammatory response as well as inhibited NLRP3 inflammasome[18].

### 1.5. Toll-Like Receptors (TLRs)

Drosophila was the first species where Toll protein was discovered during the early immune system development through dorsal-ventral patterning during embryogenesis[20,21]. Afterward, similar homologous receptors were found in mammals and named Toll-Like Receptors (TLRs)[22]. The mammalian TLRs are germline-encoded receptors that can be found localized as transmembrane or intracellular. Transmembrane TLRs are responsible for immune recognition of PAMPs and DAMPs via structural motifs, characteristically expressed by bacteria, viruses, and fungi[23]. Activation of such TLRs induces proinflammatory cytokines and upregulates co-stimulatory molecules, which are important mediators for innate and adaptive response of the immune system[24]. Figure 1.2 illustrates the structure of transmembrane TLR ligand.

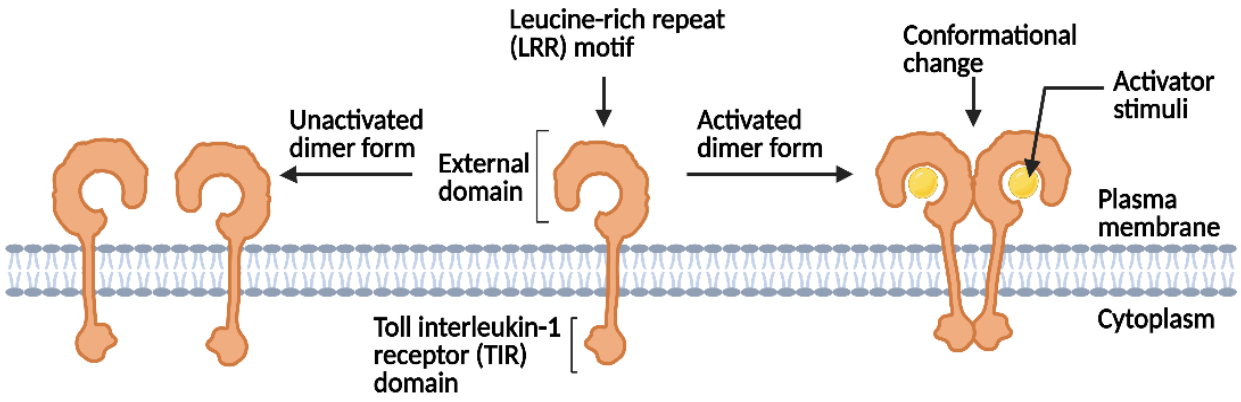


**Figure 1.2: A representative structure of membrane-bound TLR.**

The basic structure of the TLR consists of an extracellular leucine-rich repeat (LRR) domain and a cytoplasmic domain which is similar to the mammalian IL-1 receptor known as Toll Interleukin-1 receptor (TIR)[25]. TLRs exist as dimers of low-affinity complex, which upon ligand binding, initiates conformational changes and brings the two TIR-domains on the cytosolic face of each receptor into close proximity[26]. This conformational change creates the signaling platform necessary for the recruitment of adaptor molecules. As stimulating molecules bind to the LRR motif region, the cytoplasmic TIR domain initiates the intracellular downstream signaling pathways via homotypic protein-protein interaction with TIR-adaptor molecules. The figure was modified from "A representative structure of TLR" by Gao, W *et al.*[27].

Figure 1.3 illustrates human TLR signaling pathways. TLR1, TLR2, TLR4, TLR5, and TLR6 are transmembrane TLR ligands. TLR3, TLR7, TLR8, and TLR9 are expressed in intracellular vesicular compartments. TLR1 and TLR6 forms heterodimer with TLR2 for signaling (TLR 1/2 and TLR 2/6 dimers). TLR4 can activate both the MyD88-dependent and the MyD88-independent signaling pathways. TLR3 can only activate the MyD88-independent pathway, while all other TLRs signal through the MyD88-dependent pathway only.

Different TIR-adapter molecules can be mediated by TLR signaling; (i) myeloid differentiation factor 88 (MyD88), (ii) myeloid adapter-like protein (MAL or TIR Domain-Containing Adaptor Protein (TIRAP)), (iii) TIR-domain containing adaptor inducing protein inducing IFN-β (TRIF), (iv) TRIF-related adapter molecule (TRAM)[28].

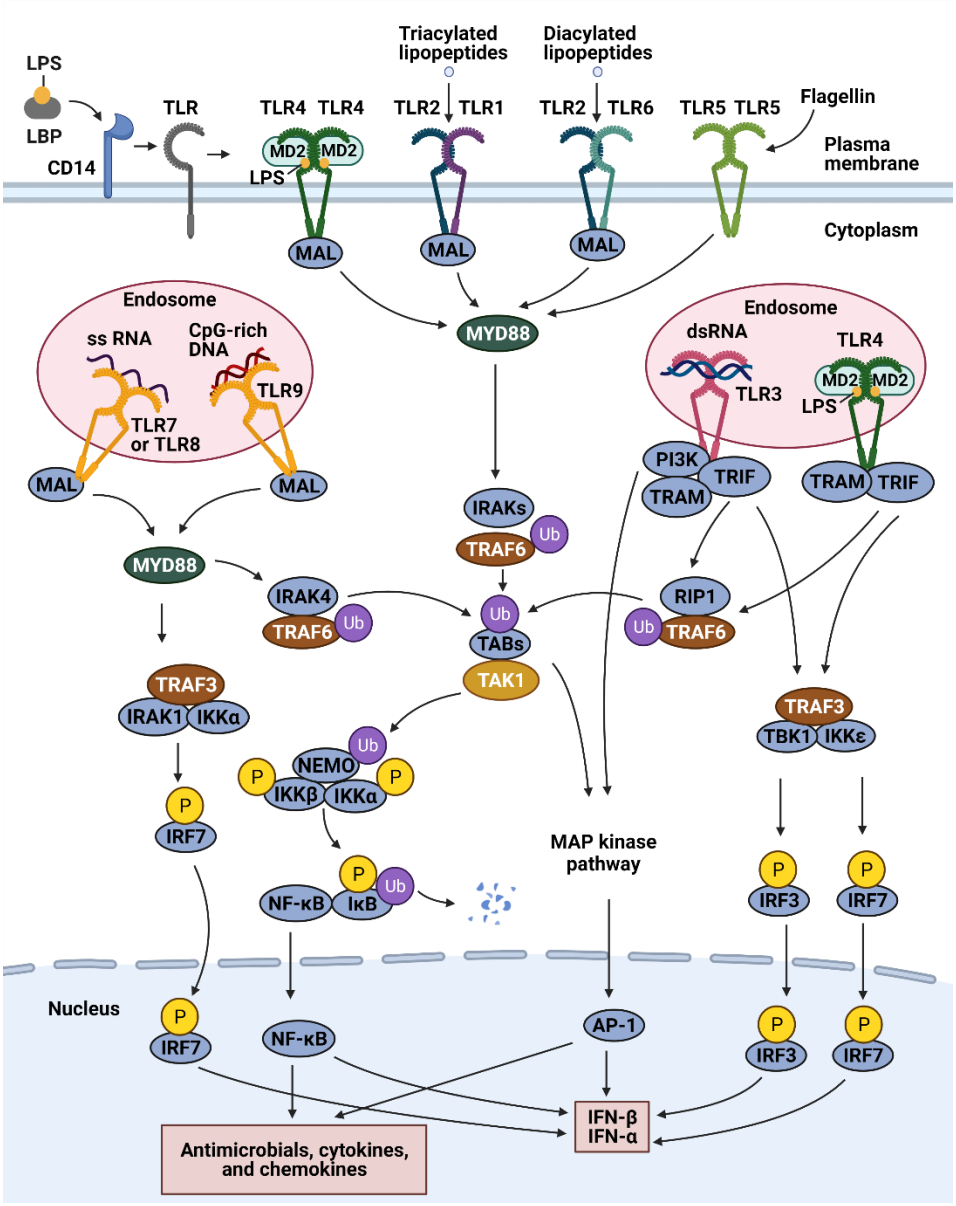


**Figure 1.3: A schematic representation of human TLR signaling pathways.**

After dimerization, transmembrane TLR 4/4, 2/1, 2/6, and 5/5 activate Mitogen-activated protein (MAP) kinase pathway and NF-κB essential modulator (NEMO) in the cytoplasm, leading to Adaptor protein-1 (AP-1) and nuclear factor kappa B (NF-κB) release in the nucleus, respectively. Endosomal TLR ligands, TLR 7/7, 8/8, 9/9, recruits Tumor necrosis factor receptor (TNFR)-associated factors (TRAFs), TRAF3, and TRAF6. The TRAF3 releases phosphor-IRF7 in the nucleus while the TRAF6 activates MAP kinase and NEMO pathway. Endosomal TLR ligand TLR 3/3 can directly activate MAP kinase pathway or recruit receptor-interacting serine/threonine-protein 1 (RIP1)-TRAF6 complex, which can activate NEMO and MAP kinase pathway. Endosomal TLR 4/4 ligand recruits RIP1-TRAF complex and TRAF3 to release MAP kinase induced AP-1, and phospho-IRF3 and phospho-IRF7 into the nucleus. The figure was modified from "TLR signaling pathways" by Pendergraft, W. F. *et al.*[29].

### 1.5.1. TLR family

13 mammalian TLRs have been identified till date, TLR1-13[30], although TLR11, TLR12, and TLR13 have not been found in humans. T**able 1.2** shows the human TLR family members, including the ligands, localization, adaptor proteins, and end products.

**Table 1.2: Overview of human TLRs, highlighting their known ligands, localization, adaptor proteins, and end products used to initiate signaling pathways, including the commonly induced cytokines**[29].

| **Toll-like receptors** | | **Ligands**[31] | **Localization** | **Adaptor proteins**[32] | **End products**[33] |
|---|---|---|---|---|---|
| TLR2 | TLR1/2 dimer | Triacyl lipopeptides | Plasma membrane | TIRAP/MyD88 | Proinflammatory cytokines |
| | TLR2/6 dimer | Diacyl lipopeptides | | | |
| TLR3 | | dsRNA | Endosome | TRIF | Proinflammatory cytokines, type I IFNs |
| TLR4 | | Lipopolysaccharide | Plasma membrane, endosome | TRAM/TRIF, TIRAP/MyD88 | Proinflammatory cytokines |
| TLR5 | | Flagellin | Plasma membrane | MyD88 | Proinflammatory cytokines |
| TLR7 | | ssRNA, base analogs | Endosome | MyD88 | Proinflammatory cytokines, type I IFNs |
| TLR8 | | ssRNA | Endosome | MyD88 | Proinflammatory cytokines, type I IFNs |
| TLR9 | | Unmethylated CpG DNA | Endosome | TIRAP/MyD88 | Proinflammatory cytokines, type- I IFNs |

### 1.5.2. TLR4

The *TLR4* gene is positioned at chromosome 9q32-33 in humans[34]. TLR expression has been found in different immune cells, monocytes, macrophages, DCs, and polymorphonuclear (PMN) cells and also expressed on many other cell types, such as osteoblasts, endothelial cells, adipocytes, kupffer cells, keratinocytes, and epithelial cells[35-37]. TLR4 activation leads to intracellular downstream signaling pathways towards inflammatory cytokine production responsible for activating the innate immune system[38]. TLR4 is well known for identifying LPS, present in many gram-negative bacteria and select few gram-positive bacteria.

### 1.5.3. TLR4 signaling

As illustrated in **figure 1.4,** upon ligand binding to the cell surface, homodimerization of TLR4 ligands initiates between their intracellular TIR-domains. This induces conformational changes in the molecule, leading to the recruitment of four TIR-domain-containing adapter molecules, which can initiate two distinct signaling pathways; MyD88-dependent signaling and MyD88-independent or TRIF-dependent signaling[39].

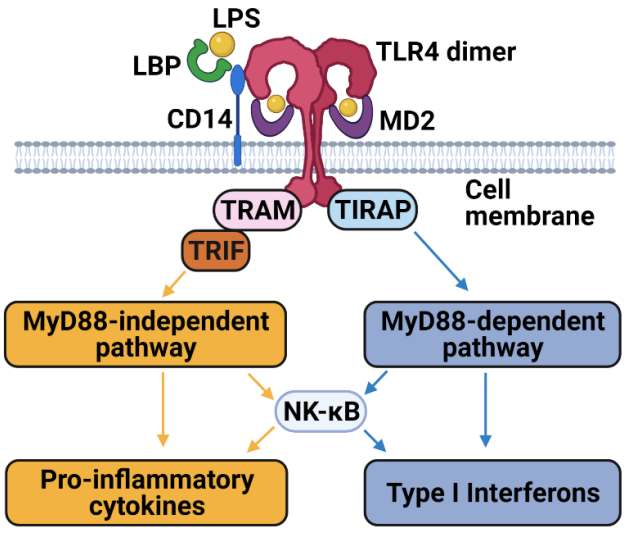


**Figure 1.4: Overview of LPS inducedTLR4 signaling pathways.**

LPB and CD14 facilitate LPS recognition, while the TLR4-Myeloid Differentiation Factor-2 (MD-2) receptor complex mediates the recognition process. The figure is modified from the "LPS/TLR4 signal transduction pathway" by Lu, Y.-C. *et al.*[39].

### 1.5.4. MyD88-independent/TRIF-dependent pathway

The TIR-domain containing TRIF-related adapter molecule (TRIF-TRAM) complex can lead to two distinct signaling pathways. In one pathway, the TRIF-TRAM complex activates NEMO and MAP kinase pathways. On the other pathway, TRIF3 recruits IL-1 Receptor-Associated Kinase 1 (IRAK1) and releases IRF3 and IRF7, as illustrated in figure 1.5.

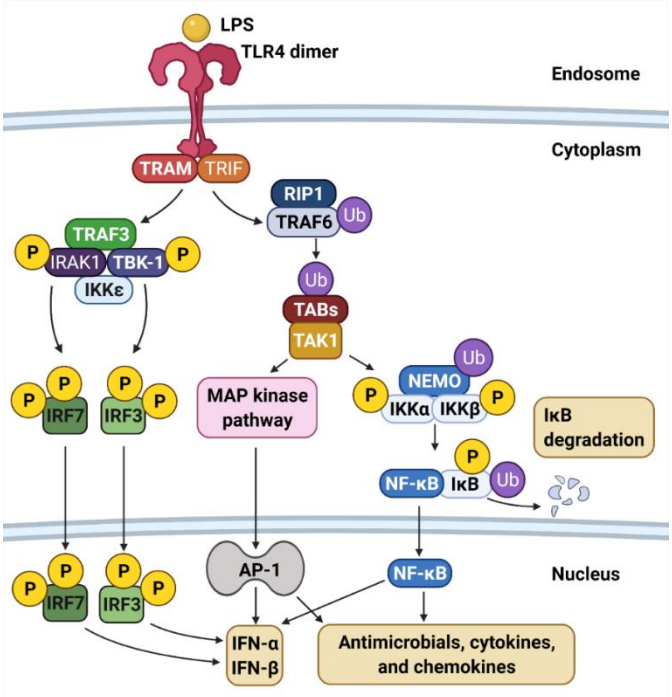


**Figure 1.5: LPS induced MyD88-independent TLR4 signaling pathway.**

TRIF-TRAM recruits RIP1 and TRAF6 adaptor protein. Upon ubiquitination of TRAF6, the RIP1-TRAF6 complex activates (TGF-β1)-activated kinase 1) TAK1 through (TAK1)-binding proteins (TABs). Further ubiquitination of TABs leads to activation of both NEMO and MAP kinase pathways. The NEMO protein complex consists of Inhibitor of NF-κB kinase subunit α (IKKα) and Inhibitor of NF-κB kinase subunit β (IKKβ). Ubiquitination of NEMO, and phosphorylation of both IKKα and IKKβ, releases NF-κB and inhibitor of nuclear factor kappa B (IκB) in the cytoplasm and inactivates IKKα and IKKβ[40]. IκB is degraded in the cytoplasm through phosphorylation and ubiquitination, releasing NF-κB into the nucleus. Ubiquitination of TABs also activates MAP kinase cascade, which activates AP-1 and releases it in the nucleus. Both the NF-κB and AP-1 proteins produce proinflammatory cytokines as well as interferons. On the other hand, the TRIF activates TRAF3, further recruiting other protein complexes: IRAK1, Inhibitor of NF-κB kinase subunit α (IKKε), and TANK-binding kinase 1 (TBK1). The complex phosphorylates and activates interferons: IRF3 and IRF7. Both interferons dimerize and move into the nucleus and induce the transcription of the IFN-α and IFN-β genes. The figure is modified from the "The MyD88-independent pathway" by Lu, Y.-C. *et al.*[39].

### 1.5.5. MyD88-dependent pathway

The MyD88-dependent signaling pathway is associated with MyD88 and MAL or TIRAP[38]. IRAKs and TRAF6 are recruited, which activates TABs and TAK1, leading to NEMO and MAPK pathway activation, similar to the MyD88-independent pathway as illustrated in figure 1.6.

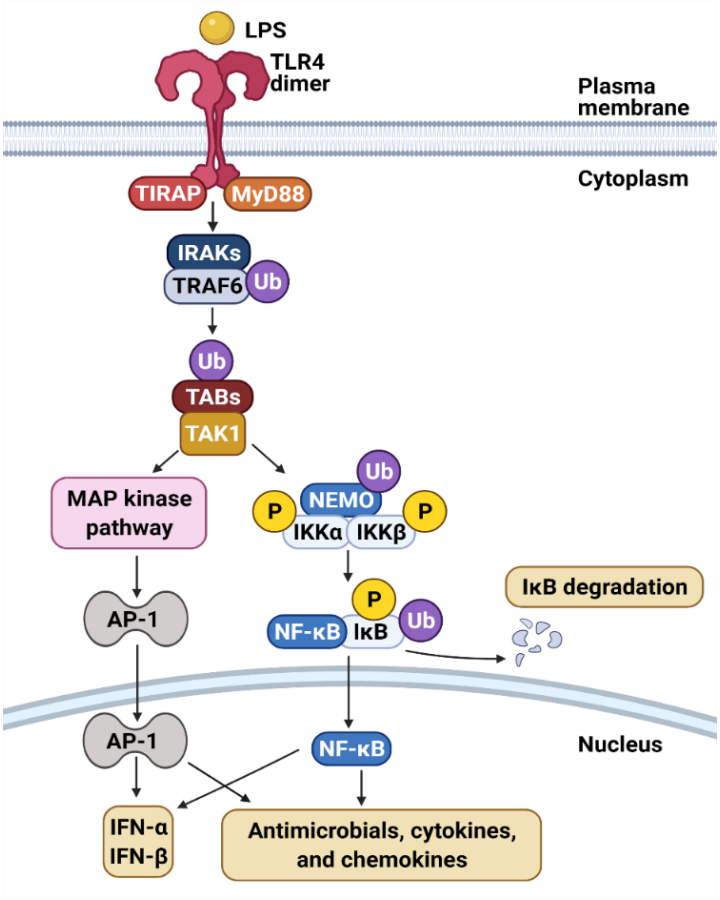


**Figure 1.6: LPS induced MyD88-dependent TLR4 signaling pathway.**

TIRAP-MyD88 signaling recruits and activates of IRAKs and the adaptor molecules TRAF6. Upon ubiquitination, IRAKs and TRAF6 activate TAK1[41]. As TABs go through ubiquitination, the TAK1 molecule initiates both NEMO and MAPK pathways for further downstream signaling. Similar to the MyD88-independent pathway, NEMO and MAPK pathway ultimately release AP-1 and NF-κB inside the nucleus, which eventually releases cytokines, chemokines, antimicrobials, and interferons[42]. The figure is modified from "The MyD88-dependent pathway" by Lu, Y.-C. *et al.*[39].

### 1.5.6. Lipopolysaccharide (LPS)

Lipopolysaccharide (LPS) is one of the most studied immunostimulatory components[43]. Originating in Gram-negative bacteria, LPS is a structural component that consists of three components: lipid A, a core oligosaccharide, and an O side chain[44,45]. The lipid A part is recognized by PRRs. LPS has been found to be associated with inflammation and sepsis[43]. However, the structure and shape of LPS are critical, as the study has found that only LPS containing conically shaped lipid A portion can act as an activator for TLR4[46].

### 1.5.7. Mimicking TLR4 signaling in macrophages with lipopolysaccharide (LPS)

Upon LPS stimulation in mammalian macrophages, a series of interactions occur with several proteins, including the LPS binding protein (LBP), CD14, MD-2, and TLR4[47]. LBP initially binds to LPS and forms a ternary complex with CD14. Afterward, the complex formation allows LPS to be transferred to the LPS receptor complex composed of TLR4 and MD-2, as illustrated in figure 1.4[48,49]. The soluble CD14 (sCD14) in plasma associates with LPS to convoy signal in cells that lack membrane-bound CD14, such as endothelial and epithelial cells. On the other hand, the membrane-bound CD14 (mCD14) allows CD14 to be membrane-proximal despite lacking a transmembrane domain[50,51]. Since anchoring of CD14 does not require any transmembrane domain, it is highly unlikely that CD14 alone conveys the signal in response to LPS. This was further established when subsequent studies found that TLR4 is the original receptor for LPS[52]. The primary role of CD14 was established later as binding to LPS and simultaneously presenting the LPS-CD14 complex to MD-2 and TLR4. During LPS stimulation, the MD-2 molecule serves as an extracellular adaptor protein which eventually activates TLR by ligand recognition. The importance of MD-2 was concreted when a study found that the presence of a mutant form of MD-2 (C95Y) abolishes LPS response completely[53]. Upon recognition of LPS, TLR4 undergoes oligomerization and recruits the essential downstream adaptors. The signal transduction has been illustrated in figures 1.4, 1.5, 1.6.

### 1.6. Monocytes and macrophages

In the event of pathogens passing through the physical and/or chemical barriers of the human body, innate immune cells immediately encounter them to prevent any occurrence of infection. In such conditions, monocytes and macrophages act as antigen-presenting cells (APCs)[54]. They serve as a cellular bridge between the innate and adaptive immune systems by engaging the pathogens at the site of infection and initiating pathogen-specific immune responses via activation of T-cells[54]. Similar to other immune cells, monocytes and macrophages also recognize pathogens, cell damage, and cell death by their PRRs[55].

Monocytes are a heterogeneous group of cells that are present in systemic blood circulation. They play a vital role in infection and inflammation by (i) removing pathogens and other particles via phagocytosis, (ii) presenting antigen to T-cell, (iii) secreting regulatory mediators such as cytokines[56,57]. Upon migration into tissues, monocytes differentiate into a diverse array of tissue-resident phagocytic cells, including macrophages and dendritic cells[58].

Monocytes from systemic circulation differentiate into macrophages once they arrive in tissues and inherit the functional properties of macrophages. The differentiation process is necessary for the active participation of the cells in the immune response. With differentiation, cells go through a magnitude of changes, such as the increase in cytoplasmic volume and the number of organelles[3]. Based on the location of the tissues, they divide into specific populations[59]. Macrophages are specialized innate cells capable of detecting and eliminating apoptotic cells, particles, and microbes through phagocytosis[54]. Macrophages release several different mediators such as cytokines, enzymes, growth factors, and oxidants. These mediators eventually regulate inflammation, host defense, and homeostasis[54]. In addition, macrophage responses towards ligands also differ, leading to different downstream signaling pathways[60]. One such PRR is the Toll-like receptor (TLR), which upon stimulation in monocytes and macrophages, show different consequences leading to a different response to pathogens[3]. Table 1.3 shows some major functions of macrophages upon PAMPs recognition[61].

**Table 1.3: Macrophage receptors associated with PAMPs recognition.**

| Receptors | Functions[62] |
|---|---|
| SR-A | Phagocytosis of bacteria and apoptotic cells, endocytosis of modified LDL, adhesion |
| CD36 | Phagocytosis of apoptotic cells, diacyl lipid recognition of bacteria |
| TLRs | Response to peptidoglycan and LPS |
| CD14 | LPS-binding protein/interaction MD-2/MyD88, TLR signaling, apoptotic cell recognition |
| CR3 (CD18/11b) | Complement receptor (C3b) mediated phagocytosis, adhesion to the endothelium |
| CCR2 | Receptor for MCP-1 |
| Dectin-1 | β-glucan receptor, fungal particle ingestion, interaction with TLR-2 |

### 1.6.1 Polarization of macrophages

As mentioned above, macrophages can adapt to a variety of functions depending on the surrounding microenvironment signals. This versatile adaptability is often referred to as the polarization of macrophages. Polarized macrophages are important for tissue repairing and homeostasis maintenance. They can produce distinct functional phenotypes as a reaction to specific microenvironmental stimuli and signals[63-65].

The polarization process utilizes arginine metabolism via two antagonistic pathways. Classically activated (M1) macrophages are characterized by iNOS expression, while alternatively activated (M2) macrophages are characterized by arginase expression[66-68]. Additionally, M2 macrophages are subcategorized into M2a, M2b, M2c, and M2d. Each of the subcategories differs in their cell surface markers, secreted cytokines, and biological functions, as illustrated in figure 1.7[69]. While M1 macrophages release cytotoxic and proinflammatory mediators in response to invading pathogens, M2 macrophages release inflammatory mediators along with growth factors with the purpose of restoring the natural homeostasis of the body[54].

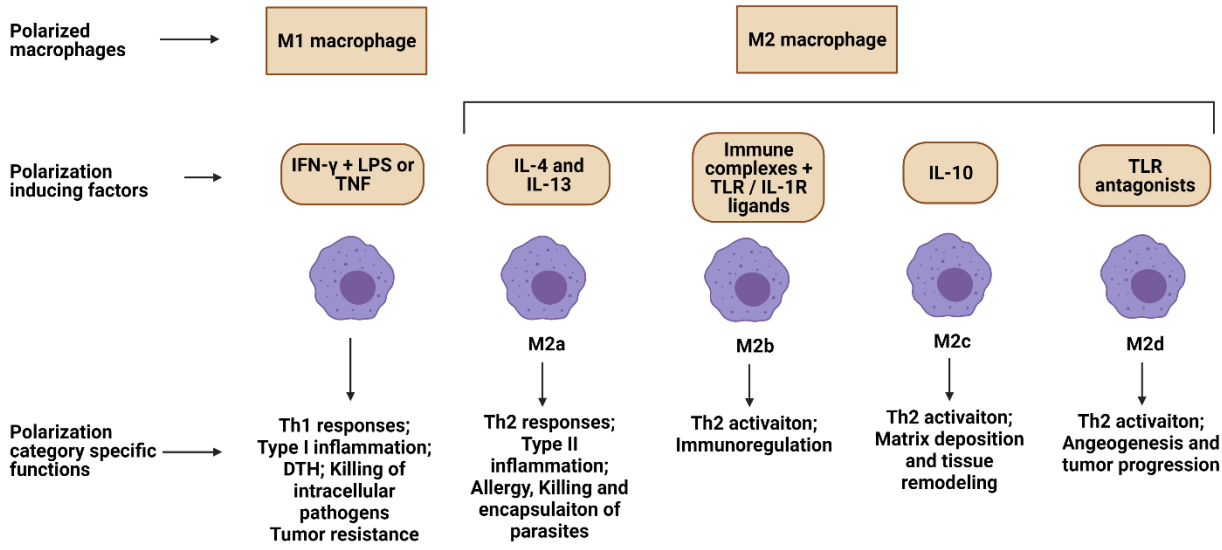


**Figure 1.7: Inducing factors and functional properties of different polarized macrophages.**

Upon activation through LPS and Th1 cytokines, macrophages polarize into M1 macrophages, which can be characterized by TLR-2, TLR4, CD80, CD86, iNOS, and MHC-II surface phenotypes. Polarized M1 macrophages attract more unpolarized macrophages into the M1 state by secreting different cytokines and chemokines such as TNF-α, IL-1β, CXCL9, etc.[70]. As a result, during M1 activation, the expression of PRRs such as TLRs and NLRs and expression of TNF-α, IL-1β, IL-6, IL-8, and IL-12 genes are upregulated[66,71]. These expressions of PRRs and genes can be controlled by regulating key transcription factors of M1. Among these transcription factors, the NF-κB pathway is involved with the regulation of M1 macrophage polarization, further regulating microbicidal and tumoricidal functions[72-74].

M2 macrophage polarization is initiated by the downstream signaling of cytokines such as IL-4, IL-13, IL-10, IL-33, and TGF-β[75,76]. IL-4 and IL-13 initiate M2 macrophage activation directly, while IL-33 acts as an amplifier by producing other type II helper T cell (Th2) cytokines[77]. The four subcategories of M2 macrophages are induced by different stimuli as follows: (i) M2a induced by IL-4 or IL-13, (ii) M2b induced by immune complexes (IC)/TLRs agonist or IL-1 Receptor, (iii) M2c induced by IL-10, and (iv) M2D induced by TLR antagonists[78,79]. The figure was modified from "The heterogeneity and characterizations of macrophages" by Wang, Y *et al.*[80].

### 1.7. THP-1 cell line as monocyte and macrophage response model

The human THP-1 cell line was first established in 1980. After investigating peripheral blood of a 1-year-old human male with acute monocytic leukemia, the research group suggested that the THP-1 cell line mimics primary monocytes and macrophages concerning a variety of criteria, such as morphology, secretory products, oncogene expression, expression of membrane antigens, and expression of genes involved in lipid metabolism[2]. Comparing with other human myeloid cell lines, such as HL-60, U937, KG-1, or HEL cell lines, differentiated THP-1 cells behaved more like native monocyte-derived macrophages regarding the criteria mentioned above[81].

The THP-1 round suspension cells express signature monocytic markers and, when exposed to phorbol-12-myristate-13-acetate (PMA), initiate differentiation[82]. The macrophages tend to acquire different shapes while the absence of a nucleus becomes more prominent. Additionally, phagocytic vacuoles become more profound, which are also localized in their cytoplasm. Cell differentiation is also associated with cell adhesion to the surface of the culture plate. Flow cytometric analysis has also found that, shortly after cell differentiation, the cell volume decreases[83]. Morphological study of newly differentiated cells suggested flat and amoeboid-shaped cells with well-developed Golgi apparatuses, rough endoplasmic reticulum, and large numbers of ribosomes in the cytoplasm[81]. The cell differentiation can also be conducted by stimulating monocytes with another reagent 1α, 25-dihydroxyvitamin D3 (vD3)[84]. Although both reagents (PMA and vD3) serve the same purpose of differentiating monocytes into macrophages, they regulate different downstream signaling pathways. While PMA recruits protein kinase C at the intracellular side of the plasma membrane, vD3 up-regulates the expression of MAPK phosphatase-1 (MKP-1)[85]. The advantage of PMA treatment over vD3 is that PMA stimulated macrophages are (i) phenotypically more mature with higher levels of adherence, (ii) has a lower rate of proliferation, (iii) has a higher rate of phagocytosis and, (iv) contains higher cell-surface CD11b and CD14[85]. Hence, PMA treated THP-1 macrophages are widely used to study macrophages. Additionally, the expression of MAP kinases has been found to be generally higher, and TLR ligands, when activated, have shown to induce comparable cytokine gene expression levels as well[86].

### 1.8. Immunometabolism

Immunometabolism focuses on intracellular metabolic pathway alterations in immune cells during activation. Both the effect of metabolic regulation on immune functions and the effect of immune functions on the regulation of metabolism are studied in immunometabolism[87]. Under different metabolic conditions, the immune system functions differently.

The mitochondrial tricarboxylic acid (TCA) cycle in aerobic organisms is responsible for releasing stored energy through a series of biochemical reactions. Through aerobic glycolysis, the cycle produces energy. In the case of highly proliferative cancer cells, they undergo metabolic reprogramming, which increases energy demand. The aerobic glycolysis cannot meet the increased energy demand threshold. To overcome such problem, the proactive cells modify the energy method to anaerobic glycolysis, a phenomenon which is known as the "Warburg effect"[88]. This metabolic alteration can support the required energy production demand for rapidly proliferating cells, and such metabolic alterations are the focus points of immunometabolism.

### 1.9. Succinate

Succinate is the anionic form of succinic acid, which is commonly found in living organisms. Succinate is produced and stored in the mitochondria[89]. The localization of succinate allows it to play a vital role in energy production, specifically, adenosine triphosphate (ATP) synthesis via the TCA cycle. Succinate has been found to be associated with inflammation, tumorigenesis as well as hypoxia-induced ischemic injury[90-92]. In a biological system, succinate can be found in two forms: cell-permeable diethyl succinate and cell non-permeable disodium succinate. Upon hydrolysis, diethyl succinate produces monoethyl succinate, and succinate acid, while disodium succinate releases succinate and sodium salt.

#### 1.9.1. Succinate in TCA cycle

In aerobic organisms, succinate originates in the TCA cycle to release stored energy through the oxidation of acetyl-CoA derived from carbohydrates, fats, and proteins. In eukaryotic cells, the TCA cycle occurs in the mitochondrial matrix, and succinate acts as a ligand for electron transport chain (ETC) complex II, supplying ATP synthase electrons to drive ETC through oxidation to fumarate.

The TCA cycle begins with the production of citrate, which rapidly undergoes isomerization and produces isocitrate. Oxidation of isocitrate yields oxalosuccinate, the first succinate species compound in the sequential reactions. Oxalosuccinate reacts with isocitrate dehydrogenase enzyme to produce α-ketoglutarate, which later goes through an irreversible stage of oxidation and decarboxylation to generate NADH and succinyl-CoA. With phosphorylation, succinyl-CoA produces succinate as a metabolic intermediate. In ordinary circumstances, succinate is further converted into fumarate through oxidation[93].

### 1.9.2. Succinate accumulation through TLR4 activation

When TLR4 is activated in macrophages, the TCA cycle is shortened, leading to decreased succinyl dehydrogenase (SDH) activity at the site of ETC complex II. Eventually, succinate oxidation is limited, leading to decreased fumarate production and increased succinate accumulation[94,95].

### 1.9.3. Succinate stabilizes HIF-1α allowing inflammatory cytokine secretion via mitochondrial ROS generation

Traditionally, HIF-1α is regulated by prolyl hydroxylases (PHDs). PHDs are inhibited upon succinate accumulation, which allows direct stabilization of the HIF-1α transcription pathway inducing inflammatory cytokines such as interleukin-1β (IL-1β) secretion in macrophages[96].

Other than the traditional inhibition of PHDs through direct stabilization of HIF-1α, succinate has been found to indirectly stabilize HIF-1α through mitochondrial reactive oxygen species (ROS) generation. Studies have found that inhibition of SDH induces HIF-1α stabilization in a ROS-dependent manner[97]. SDH is responsible for the conversion of succinate to fumarate. When mitochondria are not producing enough ATP, the co-enzyme Q (CoQ) pool decreases, which leads to the reversal of the normal direction of electron flow. In such scenario, ROS oxidizes $Fe^{2+}$ of HIF-1α into $Fe^{3+}$ [98]. Oxidation of the iron molecule indirectly limits the activity of PHDs, therefore, stabilization of HIF-1α[97].

Additionally, succinate has been found to utilize succinate receptor (SUCNR1) to induce inflammatory responses. SUCNR1 receptor is a G-protein coupled receptor (GPR91), which

activates upon binding to succinate and induces MAP kinase signaling pathway[99]. The final result is increased inflammatory cytokine production[100]. However, the type of cytokine production varies, depending on the type of species-specific cell[101].

### 1.9.4. Succinate induces "Warburg effect" in hypoxic conditions

Similar to metastatic fast-growing cancer cells, cell inflammation shows increased levels of succinate. The high level of succinate is due to the hypoxic condition, which forces oxidative phosphorylation to start instead of regular glycolysis. In a regular cellular metabolic process, glucose is metabolized to produce energy. Via glycolysis, one molecule of glucose is broken down into 36-molecules of ATP via pyruvate dehydrogenase (PDH)[102]. However, this mechanism is diverted to a different direction in an anoxic or hypoxic condition. In such situations, cells can divert pyruvate away from oxidative phosphorylation in mitochondria allowing ATP generation in a low oxygen state. Furthermore, one glucose molecule only generates two ATP molecules with the help of lactate dehydrogenase (LDH).

To meet the energy demand of the cells, cells change their metabolic profile from a low rate of glycolysis which is followed by oxidation of pyruvate by the TCA cycles, to a much lower rate of oxidative phosphorylation followed by a much higher rate of glycolysis by the lactic acid production (LDH dependent pathway). This phenomenon initiates under anaerobic conditions, and the unique high glycolytic rate and high glucose dependency are known as the "Warburg effect"[103]. Due to the increased glucose production, the cell initiates more energy production by breaking more glucose molecules. This leads to increased production of α-ketoglutarate, which eventually produces succinyl-CoA and succinate[102]. Higher accumulation of succinate stabilizes HIF-1α and increases mitochondrial ROS production, both of which acts as the driving force of proinflammatory response in macrophages.

### 1.9.5. Proinflammatory and anti-inflammatory activity of succinate

Succinate has been very well studied for its proinflammatory effects. Succinate elicits proinflammatory response through HIF-1α stabilization and subsequent IL-1β secretion as well as through the production of mitochondrial ROS[96,104]. Although the proinflammatory state of the succinate-SUCNR1 axis has been well established, contradictory behavior of anti-inflammatory

effects of succinate and SUCNR1 has also been elucidated for a variety of diseases[93]. The effect of succinate-SUCNR1 has been studied with respect to obesity and cancer, convincingly suggesting that in the tumor microenvironment, succinate can polarize tumor-associated macrophages (TAMs) into a suppressive phenotype through SUCNR1 binding[105]. One explanation for this opposing statement can be the use of two different forms of succinate; a cell-permeable form: diethyl succinate, a synthetically generated form, and another being non-permeable form disodium succinate, which upon dissolving in water releases the naturally abundant form by dissipating the sodium ions[105]. Succinate has been found to mediate anti-inflammatory activity through the SUCNR1-independent mechanism.

Additionally, SUCNR1 can also participate in decreasing succinate-induced inflammatory response. It was assumed that the minor differences in the cell culture methods such as cell line (THP-1 vs. mBMDM (mouse bone marrow-derived macrophages)), media (RPMI-1640 vs. DMEM), or fetal serum (FBS vs. FCS) might have influenced the different responses induced by succinate[104]. These dynamic inflammatory effects of succinate are highly context-specific[106].

## 2. AIM

i. To investigate the effect of succinate on TLR4 signaling through the MyD88-dependent and MyD88-independent pathways.

ii. To investigate the effect of succinate on cytokine secretion through the TLR4 signaling pathway.

iii. To investigate the regulatory effect of succinate on LPS based on TLR4 signaling pathway.

# 3. MATERIALS AND METHODS

## 3.1. THP-1 Cell culture

All experiments in the project were conducted with the THP-1 cell line, which was purchased from American Type Culture Collection (ATCC). THP-1 is a monocytic-like cell line established from a 1-year old boy with acute monocytic leukemia[2]. The cells can be identified from the characteristic presence of α-naphthyl butyrate esterase (a cytochemical marker for monocytes), phagocytic activity through Fc and C3b receptors, and lysozyme production[81].

### 3.1.1. Cell culture condition

#### 3.1.1.1. Equipment and reagents

T25 Corning® cell culture flasks with vented caps (Sigma-Aldrich, Cat. No: 430639), T75 Corning® cell culture flasks with vented caps (Sigma-Aldrich, Cat. No: 430641), T175 Corning® cell culture flasks with vented caps (Sigma-Aldrich, Cat. No: 431080), Z2 Coulter counter (Beckman Coulter), RPMI-1640 (Sigma-Aldrich, Cat. No: R8758), Fetal calf serum (FCS) (Gibco, Cat. No: 10270), L-glutamine (Sigma-Aldrich, Cat. No: G7513), Penicillin-Streptomycin solution (Sigma-Aldrich, Cat. No: P0781), β-mercaptoethanol (Sigma-Aldrich, Cat. No: 60- 24-2), Phorbol 12-myristate 13-acetate (PMA) (Sigma-Aldrich, Cat. No: P8139), Dulbecco's Phosphate Buffered Saline (PBS) (Sigma-Aldrich, Cat. No: D8537), Z2 Coulter counter (Beckman Coulter).

#### 3.1.1.2. Procedure

The THP-1 cells were cultured using complete RPMI-1640 media with 10% FCS, 2mM L-glutamine, 0.05mM β-mercaptoethanol, 100 units/ml penicillin, 0.1 mg/ml streptomycin at 5% $CO_2$ at 37 °C. In a culture flask, cells were seeded at a concentration of 200,000 cells/ml. The cells doubled every 19-26 hrs and were split every third day to ensure cell density of 550,000 to 600,000 cells/ml. Undifferentiated THP-1 cells grew in suspension as large, round single cells[2]. Before splitting the cells, they were observed under an inverted microscope to check cell dispersion.

### 3.1.2. Cell counting

THP-1 cells were counted using Z2 Coulter counter[107]. The culture flasks were gently shaken to spread out the cells evenly into the media. Then, 20 µl cell suspension was pipetted and diluted in a coulter counter container with 10 ml coulter counter diluent. The particle count range was selected from 10-19 µm. Each cell counting was performed 3X times, and the average cell number was taken for appropriate cell count.

## 3.2. Cell differentiation

### 3.2.1. Principle

THP-1 monocytic cells were differentiated into macrophages-like cells by stimulating with phorbol 12-myristate 13-acetate (PMA). Using PMA for cell differentiation results in terminal cell differentiation leading to cell proliferation arrest and increased adherence to culture plate surface[108].

### 3.2.2. Procedure

THP-1 monocytic cells were transferred to 50 ml falcon tubes from culture flasks and centrifuged at 300 x g for 10 min at room temperature. Supernatants from each tube were removed carefully without disturbing the cell pellets at the bottom of the tubes, which got rid of any dead cells floating in the supernatant. Precipitated cell pellets were resuspended using fresh complete culture media to the appropriate concentration for the experiments.

Specific concentrations of cells and reagents were used throughout the study. The concentration for resuspended cell samples was $3 \times 10^6$ cells/ml, and the concentration of PMA aliquot was 50 ng/ml.

Cells were seeded in 6-well cell culture clusters for cell differentiation. The optimum volume for each well is 2 ml. In each well, 1 ml of resuspended cell solution and 1 ml of PMA aliquot were added before incubating for 16 hrs in 5% $CO_2$ at 37 °C. After the incubation period, cells were observed using an inverted microscope to ensure cell differentiation and cell adhesion to the well surface. Upon cell differentiation, the supernatant containing PMA was replaced with fresh

complete culture media before incubating for another 48 hrs in 5% $CO_2$ at 37 °C before exposing to the experimental conditions.

Cells were differentiated for experimenting with four conditions over 5-time points: 30 min, 2 hrs, 4 hrs, 6hrs, and 24 hrs. Three wells were used for each condition as biological replicates.

### 3.3. Experimental conditions

The differentiated cells were exposed to four experimental conditions: (i) not stimulated/control (Ctrl), (ii) lipopolysaccharide (LPS) stimulation, (iii) disodium succinate (Suc) stimulation, (iv) lipopolysaccharide and disodium succinate (LPS+Suc) combined stimulation.

#### 3.3.1. Cell stimulation with experimental conditions

Aliquots of the stimulants were prepared by diluting the stimulants into complete RPMI-1640 culture media. Specific concentration of LPS, succinate, LPS + succinate combination were used for the experiments, which are as follows: (i) LPS (200 ng/ml), (ii) Suc (160 mM or 25.928 mg/ml disodium succinate), (iii) LPS+Suc (200 ng/ml of LPS + 160 mM or 25.928 mg/ml of disodium succinate)[109]. For succinate and LPS + succinate combination aliquot preparation, disodium succinate was weighted first using an electronic balance and transferred into a 50 ml falcon tube. The appropriate volume of media was added to maintain the concentration and shaken vigorously to mix the succinate with the media. For LPS + succinate, LPS was added to the Suc-media mixture. For the LPS aliquot, in a 50 ml falcon tube, LPS was added to an appropriate volume of media. For Ctrl, fresh media was used.

Before introducing the conditions to the cells, the overlaying media in the 6-well cell culture clusters were discarded. The Ctrl wells were filled with 2 ml fresh completed RPMI-1640 media, while the condition sample wells were filled with 2 ml of freshly prepared respective stimulation aliquots. All the stimulation aliquots were kept at room temperature. After stimulation, all 6-well cell culture clusters were incubated in 5% $CO_2$ at 37 °C for the designated stimulation time periods: 30 min, 2 hrs, 4 hrs, 6 hrs, and 24 hrs. To avoid any shortage, all the aliquots were prepared to an additional volume more than what was required.

### 3.4. Protein extraction

#### 3.4.1. Reagents and equipment

Dulbecco's Phosphate Buffered Saline (PBS) (Sigma-Aldrich, Cat. No: D8537), sodium dodecyl sulfate (SDS) buffer (Sigma-Aldrich), triethylammonium bicarbonate (TEAB) (Sigma-Aldrich), EDTA-Free Protease Inhibitor Cocktail (Roche, Cat. No: 11836170001), PhosSTOP Phosphatase Inhibitor tablets (Roche/Sigma, Cat. No: 04906837001), Dulbecco's Phosphate Buffered Saline (PBS) (SigmaAldrich, Cat. No: D8537), 2.5 cm cell scraper, digital sonifier (BRANSON).

#### 3.4.2. Principle

Cell membrane lysing allows the protein to be released from the inside of the cells. Cell lysis buffer ruptures the cell membrane integrity and releases the proteins into the lysis buffer, which can be collected for protein estimation.

In this project, sodium dodecyl sulfate (SDS) was used to perform the cell lysis method where the combined lysis buffer contained 4% SDS, triethylammonium bicarbonate (TEAB) buffer, and Mili-Q water. Being an anionic detergent, the SDS buffer breaks hydrogen bonds within the proteins and denatures secondary and tertiary structures. TEAB buffer helps to digest trypsin as well as to adjust the pH of buffer for protein quantification[110,111]. Additionally, EDTA-Free Protease Inhibitor Cocktail and PhosSTOP Phosphatase Inhibitors are added to the combined lysis buffer to inhibit protein dephosphorylation. Adhered cells are scraped along with the lysis buffer followed by heating which allows the proteins to be completely denatured. Heating also allows evaporation of access TEAB buffer. Centrifugation is required to pellet unwanted cell debris and permit clarified lysate recovery. Sonication was conducted next, to rapture the cellular membrane integrity properly.

#### 3.4.3. Procedure

Cell lysis buffer was carefully prepared to a volume of 20 ml by mixing 10% sodium dodecyl sulfate (SDS) buffer (8 ml to make 4% SDS), 50 mM TEAB buffer (1 ml), and Mili-Q water (q.s. to 20 ml which is 11 ml). 2X EDTA-Free Protease Inhibitor Cocktail tablets and PhosSTOP

Phosphatase Inhibitor tablets were added. The lysis buffer was kept in an aluminum-wrapped tube as TEAB is sensitive to light.

After exposing the cells to each stimulation for designated time periods, the protein extraction step was performed. First, supernatant from all wells was discarded. To avoid any contamination, overlaying solutions from each media were discarded using new pipette tips for each well. Afterward, each of the wells was washed 3X with 2 ml/well cold Dulbecco's Phosphate Buffered Saline (PBS), and the supernatants were discarded after each wash.

After washing with PBS, 200 µl of combined lysis buffer was added to each cell well. The lysis buffer was covered thoroughly on the well surface, which was scraped properly with a 2.5 cm cell scraper. The samples were collected in separate Eppendorf tubes and were kept in a heating block for 10 min at 90 °C followed by centrifugation at 10,000 rpm at 4 °C. Afterward, each of the samples was sonicated using a digital sonifier (BRANSON) for 30 sec with 5 sec pulse-on and 5 sec pulse-off. In between each sample sonication, the sonifier rod was washed with 70% ethanol and $H_2O$, respectively. The samples were then kept in a heating block for 10 min at 90 °C followed by centrifugation at 10,000 rpm at 4 °C and stored at -20 °C freezer pending protein estimation.

### 3.5. Total protein estimation

#### 3.5.1. Reagents and equipment

Pierce™ BCA protein assay kit (thermoscientific), iMark™ microplate reader (Bio-Rad, California, US).

#### 3.5.2. Principle

For the protein estimation step, in this project Thermo Scientific™ Pierce™ BCA Protein Assay Kit was used[112]. The kit is detergent-compatible, ideal for this project since the combined cell lysis buffer contains detergent; SDS. For the colorimetric detection and quantitation of total protein, the kit uses bicinchoninic acid (BCA). The assay method reduces $Cu^{+2}$ to $Cu^{+1}$ by protein in an alkaline medium and detects the $Cu^{+1}$ ion using BCA containing reagent[112,113]. The color shift can be observed from light green to purple, where the purple color signifies chelation of two molecules

of BCA with one $Cu^{+1}$ ion. The color shift can then be detected by absorbance measurement, which allows the estimation of total protein.

### 3.5.2. Procedure

Previously collected cell lysates were retrieved from -20 °C freezer and heated at 90 °C before protein estimation. The samples were diluted using Mili-Q water to a ratio of 1:2, and total protein was estimated following the manufacturer's microplate procedure protocol; Pierce™ BCA protein assay kit in a 96-well flat-bottom plate. The standard curve dilution was performed following the manufacturer's protocol (Supplementary table 1). The plate was incubated in the dark at 37 °C for 30 min before preparing the BSA standard curve according to the protocol[112]. Using iMark™ microplate reader, the absorbance of the samples was measured at 570 nm wavelength[114]. Each sample was added as biological replicates (n = 3) in the 96-well flat bottom plate, and the average concentration for each sample was taken for further calculation.

## 3.6. Western blot

Western blot was performed in this project to investigate the effects of different conditions (i.e., Ctrl, LPS, succinate, LPS + succinate combination) on TLR4 protein expression. Additionally, western blot was performed to study the downstream signaling pathways of TLR4 by observing the protein expression of phospho-p.38MAPK (p.p38MAPK) and phospho-IRF-3 (p.IRF-3) with the help of β-actin (housekeeping antibody) and Goat anti-rabbit immunoglobulins HRP (secondary antibody).

### 3.6.1. Reagents

Dithiothreitol (DTT) (Applied Chemistry, Cat. No: A3668.0050), NuPage™ LDS Sample Buffer (4X) (Invitrogen, Cat. No: NP0007), NuPage™ 4-12% Bis-Tris Protein Gels, 10-well (Invitrogen, Cat. No: NP0321Box), NuPage™ 4-12% Bis-Tris Midi Protein Gels, 20-well (Invitrogen, Cat. No: WG1402BOX), NuPage™ MOPS SDS Running Buffer (20X) (Invitrogen, Cat. No: NP0001), SeeBlue® Plus2 Pertained Standard (Invitrogen, Cat. No: LC5925), MagicMark™ XP Western Protein Standard (Invitrogen, Cat. No: LC5602), iBlot™ 2 Transfer Stacks, nitrocellulose, mini

(Invitrogen, Cat. No: IB23002), iBlot™ 2 Transfer Stacks, nitrocellulose, regular size (Invitrogen, Cat. No: IB23001), TBS-T (Tween-20 (Sigma, Cat. No: P1379-500ML), Bovine Serum Albumin (Sigma, Cat. No: A7906-500g), SuperSignal™ West Femto Maximum Sensitivity Substrate (Invitrogen, Cat. No: 34096), LI-COR Odyssey® Fc Imaging System, Image Studio Lite Ver 5.2.

The following antibodies in **Table 3.1** were used to perform western blotting in this project.

**Table 3.1: Primary and secondary antibodies used in western blot.** Phosphorylated proteins are denoted with the prefix "p".

| Antibody | Molecular weight (kDa) | Antibody type | Host species | Clonality | Manufacturer | Product number |
|---|---|---|---|---|---|---|
| p.p38MAPK | 43 | Primary | Rabbit | Monoclonal | Cell Signaling | 4511S |
| p.IRF3 (S396) | 47 | Primary | Rabbit | Monoclonal | Cell Signaling | 29047S |
| β-actin | 42 | Primary | Rabbit | Polyclonal | Cell Signaling | 8457S |
| Goat anti-rabbit immunoglobulins HRP | 44 | Secondary | Goat | Polyclonal | Cell Signaling | 7074S |

### 3.6.2. Principle

Western blot is a semi-quantitative method used for the detection and analysis of proteins in a given sample (i.e., cells, tissues). Cell lysis buffer allows the membranes to solubilize and separate the proteins from non-soluble components of the samples. After samples are lysed, total protein is estimated, and the volume of samples is calculated for a specific amount of protein in each sample. The samples with an equal amount of proteins are then detected through gel electrophoresis and western blotting.

The gel electrophoresis system separates the samples by utilizing neutrally charged, thermo-stable, and transparent polyacrylamide gel. Depending on the size and molecular weight (MW) of the proteins, the pore size in the gel can be made smaller or larger. The concentration of polyacrylamide in the top (stacking) part of the gel and the bottom (resolving) part of the gel can

also vary. Usually, the polyacrylamide concentration of stacking and resolving gel is 4% and 4-12%, respectively, which allows proteins with smaller sizes and lower molecular weight to migrate faster than the big and heavy proteins[115].

The protein samples are prepared by the addition of lithium dodecyl sulfate (LDS) and dithiothreitol (DTT). LDS is a slightly alkaline sample buffer that allows the maximum activity of the reducing agent for protein denaturation[116]. Being a reducing agent, DTT disrupts the disulfide bonds between cysteine residues. This mixing process reduces sample proteins at the millimolar level and denatures the remaining tertiary and quaternary structure of the protein[116].

The prepared depolymerized samples are then heated, which allows negative charge accumulation and denaturation of the proteins. When connected to an appropriate power supply, the negatively charged proteins from the top of the gel will travel towards the positive electrode, connected at the bottom of the gel[115]. In addition**,** dyes are used as molecular ladders for quantification of the proteins later. The SeeBlue® Plus2 pertained standard dye allows monitoring of protein migration during gel electrophoresis by creating protein size-specific colored bands[117]. Additionally, MagicMark™ XP western protein standard dye allows detection of both chemiluminescent substrates and fluorescent secondary antibodies during band/image development[118].

Apart from connecting to a power supply with adjusted voltage, the system also requires a running buffer, which works as a source of electric conductance. For relatively larger proteins (> 30 kDa), 3-(N-morpholino) propanesulfonic acid (MOPS) running buffer is used. The gradient gel separates small- to medium-sized proteins through migration of SDS-bound depolymerized proteins towards the anode at the bottom of the system chamber[115]. While the gel buffer provides a slightly acidic pH of 6.4, the MOPS buffer provides a slightly basic pH of 7.3-7.7 and neutralizes the system environment reducing the chance of further protein degradation[119]. Since the stacking gel has a lower concentration of gel than the resolving gel, a lower voltage is provided at the beginning of the experiment and is gradually increased later. This also prevents the gel from melting and sticking to the gel template wall[115].

Upon protein separation on the gel, they are transferred onto either nitrocellulose or polyvinylidene difluoride (PVDF) membranes. For proteins larger than 20 kDa, nitrocellulose membrane is preferred due to its high protein-binding affinity and ability of protein immobilization through hydrophobic interaction[115]. Furthermore, they are cost-efficient and do not require pre-staining.

Proteins from the gel can be transferred to a membrane in either semi-dry or wet conditions. The semi-dry method is less time-consuming, as electricity is directly conducted to the gel and membrane. For the wet transfer method, both the gel and the membrane are placed between filter paper and sponges and submerged into a transfer buffer. Electrode plates are used for electricity conduction through the transfer buffer into the gel and membrane, allowing protein transfer onto the membrane. Close contact between gel and membrane ensures efficient protein transfer[115].

After protein transfer to the membrane, the reacted sites on the membrane are blocked to avoid unnecessary protein-antibody interaction during incubation. 5% bovine-serum albumin (BSA) or nonfat dried milk diluted in TBS-T are commonly used blocking agents. Nonfat dried milk is preferred due to its cost efficiency and wide availability. However, the nonfat dried milk contains several proteins, which can cause unwanted interaction with the blotted proteins on the membrane and interfere with the assay results. On the other hand, 5% BSA contains only albumin, which increases selectivity and control over the blocking process. Furthermore, using BSA as a blocking agent allows the antibodies to be reused in case the blot yields poor result. A similar preference can be seen towards TBS-T over PBS-T wash buffer when using alkaline phosphatase-conjugated secondary antibodies. This is due to the fact that PBS-T can interfere with the normal functions of alkaline phosphate[115].

Following the blocking step, protein-containing membranes are incubated in the primary antibody specific for the protein of interest. While monoclonal antibodies yield lower background noise due to specificity towards a single epitope, polyclonal antibodies can recognize a target through several epitopes with higher affinity but with higher background noise. Membranes are rinsed properly in TBS-T washing buffer before incubating with secondary antibody to minimize background noise by washing off unbound antibodies. Furthermore, since the washing buffer is neutral, it also allows the antibodies to be used multiple times. The choice of enzyme-conjugated secondary antibody depends on the species in which the primary antibodies are raised in. As a conjugated enzyme, Horse radish peroxidase (HRP) is extensively used.

In case the molecular weight of the antibodies used overlap each other, stripping for reprobing method can be used. Stripping removes primary and secondary antibodies from a western blot membrane. Mild stripping can be performed by a combined stripping buffer of glycine, SDS, and Tween 20, while a harsh stripping buffer can be conducted using a combined stripping buffer of

SDS, Tris HCL, and β-mercaptoethanol[120]. Ideally, membranes were submerged in stripping buffer and incubated at 50-60 °C for 15-20 min. However, it should be noted that over stripping can also remove the blotted proteins from the membrane. After stripping, the membranes need to be adequately washed with TBS-T or PBS-T wash buffer to neutralize the membrane, which also helps to avoid contamination of antibodies.

For image development, signal enhancers are used to increase the protein band signal intensity. One such reagent is the SuperSignal™ West Femto Maximum Sensitivity Substrate. The substrate contains luminol which is oxidized in the presence of HRP and peroxide, allowing easy visual detection of protein[121].

In this project, NuPage™ 4-12% Bis-Tris Midi Protein Gels were used as the gel electrophoresis system. NuPage™ LDS Sample Buffer (4x) and DTT were used for protein denaturation. SeeBlue® Plus2 Pertained Standard and MagicMark™ XP Western Protein Standard were used as molecular weight ladder. MOPS running buffer was used along with the TBS-T washing buffer. Proteins from the gel were transferred to the nitrocellulose membrane through the semi-dry method using iBlot™ 2 Transfer Stacks. Membranes were incubated in 5% BSA for blocking unwanted reaction sites. p.p38MAPK and p.IRF-3 were used as primary antibodies, while β-actin was used as a housekeeping antibody, and Goat anti-rabbit immunoglobulins HRP was the secondary antibody. Stripping was performed using a combined stripping buffer of SDS, Tris HCL, and β-mercaptoethanol. SuperSignal™ West Femto Maximum Sensitivity Substrate was used to develop the image in the LI-COR Odyssey® Fc Imaging System, and images were analyzed by Image Studio Lite Ver 5.2.

### 3.6.3. Procedure

Cell samples that have gone through the protein estimation assay are prepared for protein expression analysis by western blot. After total protein estimation, the sample volume required for 20 μg of protein was calculated. 20 μg protein in each sample was loaded in each well of the gel for gel electrophoresis.

Samples were heated prior to SDS-PAGE sample preparation. 4X LDS and 10% 1 M DTT were added to each sample. Samples were mixed with vortex before heating at 90 °C for 10 min and centrifuged at 10,000 rpm for 2 min.

Samples were loaded into ready-made NuPAGE 4-12% Bis-Tris gels. SeeBlue® Pre-Stained Protein Standard and MagicMark™ XP Western Protein standard were used as molecular ladders. NuPAGE gel electrophoresis system was assembled according to manufacturer's protocol[116]. 1 X MOPS running buffer was added to submerge the wells, and water was used in the isolated tank to avoid overheating.

The system was run at 80 V for 30 min followed by 180 V for 90 min. Proteins from the gel were transferred to a nitrocellulose membrane by the semi-dry method using the iBlot® 2 Gel Transfer Device. Blotting was done in three steps: 20 V for 2 min, 23 V for 5 min, and 25 V for 2 min.

The nitrocellulose membranes were washed with TBS-T and blocked with 5% BSA for 1 hr. The membranes were washed with TBS-T buffer 3X 10 min in between incubation with primary antibodies overnight at 4 °C and secondary antibody at room temperature for 1 hr. β-actin was used as the internal control. HRP-conjugated antibody was used as the secondary antibody. All antibodies were diluted according to manufacturers' protocol. Antibody stripping was conducted at 60 °C for 15 min.

SuperSignal™ West Femto Maximum Sensitivity Substrate was used for signal amplification during image development. Signal was detected on LI-COR Odyssey® Fc Imaging System, and band quantitation was done using Image Studio Lite Ver 5.2.

### 3.7. Reverse-transcription polymerase chain reaction (RT-qPCR)

In this project, RT-qPCR was performed to investigate TLR-4 mediated mRNA expression levels of the genes *TNF-α*, *IL-1β*, *MMP9*, and *TGF-β1*. Additionally, amplification *18S*, *ACTB*, *GAPDH*, and *TBP* genes were also investigated for the selection of endogenous control.

#### 3.7.1. Reagents

QiAzol (Qiagen, Cat. No: 79306), Dulbecco's Phosphate Buffered Saline (PBS) (Sigma-Aldrich, Cat. No: D8537), Direct-zol RNA Miniprep Kits (ZYMO Research Cat. NO: R2050), Zymo-Spin™ IICR Spin Column, RNeasy Mini Kit (Qiagen, Cat. No: 74106), Ethanol absolute (VWR Chemicals, Cat. No: VWRC20821.296), NanoDrop® ND-1000, MicroAmp® 8-Tube Strip (Thermo Fisher, Cat. No: N8010580), High-Capacity RNA-to-cDNA™ Kit (Thermo Fisher, Cat.

No: 4387406), NEB 1 kb DNA ladder (Biolabs® Inc., Cat. no: N3232L), UltraPure™ TAE Buffer (Cat. No: 15558042), GelRed® 10,000X in water (catalog no. 41003), C1000™ Thermal Cycler, PerfeCTa® SYBR® Green FastMix®, ROX™ (Quantabio Cat. No: 95073-250), MicroAmp® Fast 96-Well Reaction Plate (Thermo Fisher, Cat. No: 4346907).

### 3.7.2. Principles

#### 3.7.2.1. RNA extraction, purification, and quantification

Extraction and purification of RNA from a sample is one of the crucial steps in RT-qPCR since it can affect all the following steps. The aim of the extraction process is to isolate only the RNA from cell lysates. The process stabilizes the RNA molecule by inhibiting RNase activity, preserving RNA structure with maximum yield in addition to removal of compounds that can interfere with the enzymatic activities during cDNA synthesis and qPCR procedure.

In this project, QIAzol™ lysis reagent has been used for cell lysis, and Direct-zol™ RNA MiniPrep Kit has been used for RNA purification[122]. The QIAzol™ lysis reagent is a phenol/guanidine-based lysis buffer that utilizes the combination of organic extraction and chaotropic disruption for efficient lysis. The organic extraction steps remove both protein and DNA, leaving the RNA behind. DNase I treatment during RNA isolation can still leave residual contaminating DNA in the isolated RNA. DNase treatment can increase the purity of the isolated RNA. The lysed samples are mixed with an equal volume of 96% ethanol and transferred to a Zymo- Spin™ IICR Spin Column. Several steps of centrifugation follow, for the binding of the RNAs to the silicate membrane of the column, successive washes with different buffers to remove salts. The RNA is finally eluted in nuclease-free water, which prevents any interference during reverse transcription.

The RNA samples are then analyzed using a UV spectrophotometer. In this project, NanoDrop® ND-1000 has been used to measure RNA concentration and purity. In 1 µl of the sample, the spectrophotometer measures the absorbance at 230, 260, and 280 nm. Then the software provides a ratio that we interpret. Typically, “pure” RNA shows 260/280 and 260/230 ratios higher than 2.0.

Contaminants from inefficient extraction (presence of proteins) or from different reagents used in extraction protocol such as phenols, guanidine, etc. can result in lower 260/280 and 260/230 ratios. Washing with RNA wash buffer and final elution in DNase/RNase-free water should be done carefully.

#### 3.7.2.2. Reverse-transcription (RT)

Total RNA is converted by reverse transcriptase into a single-stranded complementary DNA (cDNA), which is eventually amplified in the PCR step. The RT is commonly found in retroviruses that have RNA-dependent DNA polymerase. In this project, High-Capacity RNA-to-cDNA™ Kit has been used for cDNA synthesis[123]. The RT reaction mix is prepared by mixing enzyme mix and RT buffer mix.

Incubation at 37 °C for an hour allows the annealing of the primers to the RNA and the DNA polymerization. The enzyme is deactivated at 95 °C for 5 min, and the synthesized cDNA samples are stored at -20 °C.

#### 3.7.2.3. RT-qPCR

The polymerase chain reaction (PCR) can amplify specific sequences within a DNA or cDNA template.

Typically, qPCR consists of a series of repeated temperature changes known as thermal cycles. Each thermal cycle consists of 3 steps: denaturation, annealing, and extension, where the temperature varies. During the denaturation step, the incubation temperature is high (95 °C), which allows the melting of double-stranded DNA into single-strands and loosens secondary structure in the single-stranded DNA. In the annealing step, the temperature is decreased below the melting temperature of the primers so that the complementary sequences can hybridize. Extension is the final step where the optimal temperature (72 °C) is set for DNA polymerization. The primer extension can occur up to a rate of more than 60 bases per second. The temperature steps and the length of each step depend on different parameters such as annealing temperature of the primers, length of the sequence to amplify, composition in based pairs, etc.[124]. A qPCR reaction runs for 40 thermal cycles. The primers are designed in such a way that the amplicon is small, on purpose,

to allow a short amplification time. The extension step can be combined with the annealing step, and the temperature can be optimized to 60 °C[125]. Since the cDNA is created separately (two-step RT-PCR), it can be reused to amplify other genes of interest for later analysis[126].

The result is traditionally obtained at the end of the PCR, and the PCR product or amplicon is analyzed using agarose gel electrophoresis: the PCR product migrates according to the size of the sequence, and DNA intercalant is used to reveal the DNA under UV light. This analysis is also called "endpoint" PCR. Nowadays, the amplified sequence can be detected by an instrument capable of thermal cycling and fluorescence detection and is called real-time PCR.

In this project, the fluorescence is detected using SYBR Green method. When SYBR green dye is added to a sample, it immediately binds to all cDNA present in the sample. As each PCR cycle amplifies the target sequence, the dye binds to each new copy of the cDNA, and this increases the fluorescence intensity proportionally to the amount of amplified PCR products. Since the dye binds to any amplified product, false-positive signals can be generated from binding to nonspecific DNA sequences. So, primers should be designed carefully not to amplify any non-target sequences. Furthermore, melting curves should be analyzed to ensure amplification of the target's sequence only. The real-time quantitative PCR (qPCR) correlates to the amount of template loaded in the reaction to the fluorescence level measured at each cycle. By analyzing the reactions during the linear phase of the amplification, the initial quantity of the target can be determined with great precision[125].

In this project, a two-step reverse-transcription quantitative polymerase chain reaction (RT-qPCR) has been used to detect TLR4-dependent changes in cytokine level before and after treatment of THP-1 cells with LPS, succinate, and LPS + succinate combination. For cDNA synthesis in the reverse transcription step, High-Capacity RNA-to-cDNA™ Kit was used, while PerfeCTa® SYBR® Green FastMix®, ROX™ was used as the reagent in the PCR step.

Both the absolute and relative amount of mRNA in a sample can be determined by the $C_T$ value. The $C_T$ value corresponds to the number of thermal cycles at the threshold level arbitrarily defined in the linear phase of the amplification. The relative gene amplification cycle was measured using $\Delta\Delta C_T$ method. The fold change (Rq value) is a representation of the mRNA expression level of the targeted genes. The fold change is obtained by normalization with the endogenous control gene

and the sample of reference or calibrator. The equations used for calculating fold change are mentioned below:

$\Delta C_T = C_{T\ \text{gene of interest}} - C_{T\ \text{endogenous control}}$

$\Delta\Delta C_T = \Delta C_{T\ \text{sample}} - \Delta C_{T\ \text{calibrator}}$

$Rq = 2^{-\Delta\Delta CT}$

The endogenous controls are stably expressed across experimental conditions regardless of cell treatment. The calibrators are un-stimulated samples to which other stimulated samples are compared.

### 3.7.3. RT-qPCR Procedure

THP-1 cells were seeded and treated in a similar process as discussed previously. Upon 4 hrs incubation after condition treatment, cells were lysed and RNA was extracted using QIAzol™ lysis reagent[127].

Extracted RNA was then isolated using Direct-zol RNA Miniprep Kits[128]. Using NanoDrop® ND-1000, purity of the isolated RNA samples was tested, followed by RNA quantification to calculate RNA concentration.

For cDNA synthesis, samples were prepared in MicroAmp® 8-Tube Strip and placed in C1000™ Thermal Cycler, and the program was set as 37 °C 60 min, 97 °C 5 min, and 4 °C hold. Prepared cDNA samples can be stored at -20 °C.

For qPCR, master mix aliquot was prepared for each sample by mixing SYBR green buffer, nuclease-free water, forward primer, and reverse primer[129]. cDNA samples were added to the respective master mixes in 96-well PCR plate. The plate was gently tapped, and a clear adhesive sticker was placed on the whole plate and sealed properly. The plate was centrifuged at 4 °C for 5 min before the final 40 cycle PCR run in StepOne™ RT-PCR system.

*18S*, *ACTB*, *GAPDH*, and *TBP* were analyzed first for the selection of endogenous control. Four genes of interest: *TNF-α*, *IL-1β*, *MMP9*, and *TGF-β1* were analyzed. Mean of $C_T$ value was calculated to analyze the gene amplification based on the number of PCR cycles. $R_q$ value was

calculated to analyze the relative mRNA expression of the genes. The sequence of the forward and reverse primer of all 8 genes are included in supplementary table 2.

To analyze the primer specificity, gel electrophoresis was performed with PCR products. 5 µl of PCR products and 5 µl of 1 kb ladder (NEB) were loaded in a 2% agarose gel stained with 1:100,000 GelRed, and samples were allowed to migrate for 1 hr at 100 V.

# 4. RESULTS

## 4.1. Succinate strongly induces TLR4 signaling through MyD88-dependent pathway

LPS is known to induce inflammatory and proinflammatory activity through initiating different TLR4 signaling pathways. However, succinate plays a controversial role since both inflammatory and anti-inflammatory response has been found in the previous studies[130,131]. To determine which pathways are activated by succinate and whether succinate induces inflammatory or anti-inflammatory activity over time, the effects of LPS, succinate, LPS + succinate combination treatment on TLR4 signaling was investigated through western blotting with signaling pathway-specific antibodies: p.p38MAPK (specific for MyD88-dependent pathway) and p.IRF-3 (specific for MyD88-independent pathway). As shown in figure 4.1 (B-F), all conditions generated strong TLR4 signaling through the MyD88-dependent pathway (TLR4-p.p38MAPK interaction). For the MyD88-independent pathway (TLR4-p.IRF-3 interaction), LPS generated moderate signaling early through TLR4 activation and succinate had no significant effect. This finding suggests that, plasma membrane-bound MyD88-dependent pathway is strongly induced by LPS, succinate and LPS + succinate combination. And, the endosomal MyD88-independent pathway is activated only by LPS, while succinate, LPS + succinate combination has no effect on it.

**(A)**

| Day 1 | Day 2 | Day 3 | Day 4 | Day 5 |
|---|---|---|---|---|
| • Cell seeding with PMA | • Change media | | • Treat with conditions<br>• Cell lysis | • Cell lysis |

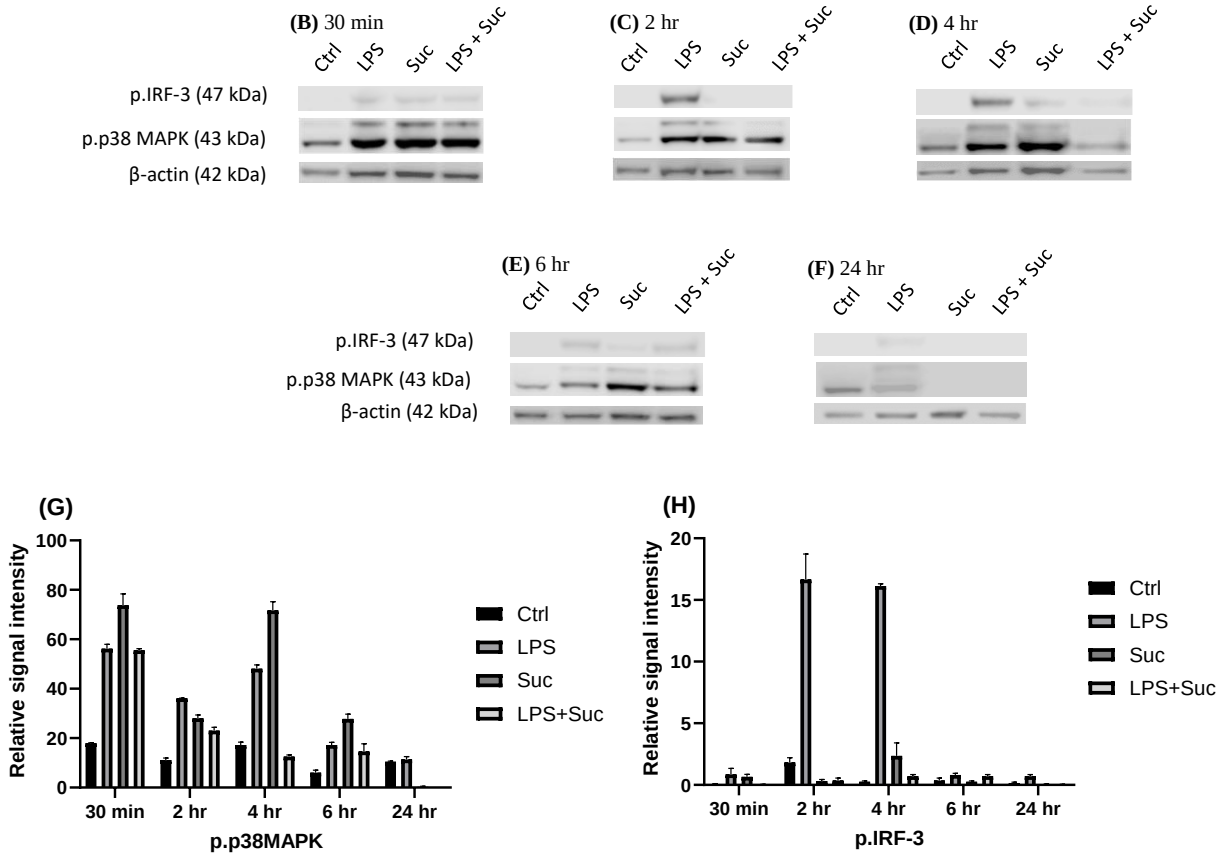


## Figure 4.1: Succinate-LPS crosstalk dampens TLR4 signaling through both MyD88-dependent pathways.

**(A)** THP-1 monocytic cells ($3x10^6$ cells/well) were differentiated with PMA (50 ng/ml) to macrophages after 16 hr incubation before introducing fresh assay media and incubation for 48 hr. Cells were treated with to 4 conditions: not-stimulated (Ctrl), LPS (200 ng/ml), Suc (160 mM), LPS+Suc (200 ng/ml, 160 mM, respectively), and incubated for 30 min, 2 hrs, 4 hrs, 6 hrs, and 24 hrs time points. **(B-F)** represents developed western blot image after incubation with p.p38, p.IRF-3, and β-actin, and goat anti-rabbit HRP over 30 mins, 2 hrs, 4 hrs, 6 hrs, and 24 hrs time point. **G)** and **H)** represents relative signal intensity of p.p38MAPK and p.IRF-3 after image development, respectively. Error bars in **(G-H)** represent standard deviation for biological replicates (n = 3).

### 4.2. Succinate-LPS crosstalk probably regulates LPS-induced MyD88-dependent TLR4 signaling.

After establishing the effect of succinate over TLR4 signaling pathways, an investigation was necessary to understand how LPS and succinate affect protein expression over time. The relative signal intensity of different conditions over 5-time points shows an overall TLR4 signaling expression difference between p.p38MAPK and p.IRF-3 induced pathways. Succinate-induced MyD88-dependent TLR4 signaling is more profound compared to the LPS and LPS + succinate combination. Although lone LPS and lone succinate induced strong TLR4 signaling, combination of LPS and succinate consecutively dampened the signaling intensity over time. On the other hand, only LPS was able to induce MyD88-independent TLR4 signaling. Additionally, protein expression was insignificant at later time points (6 hrs and 24 hrs) for p.IRF-3-TLR4 interaction. The results suggest that succinate-LPS crosstalk dampens; probably regulates LPS-induced MyD88-dependent TLR4 signaling.

### 4.3. Primer specificity analysis of RT-qPCR.

To understand inflammatory cytokine production through LPS, succinate, LPS + succinate combination induced MyD88-dependent TLR-4 pathway, mRNA expression level of genes were analyzed using RT-qPCR method. To do so, first, the specificity of the primers were checked. As illustrated in figure 4.2, the melting curves generated from the PCR run has been analyzed, and the presence of amplicon-specific peaks was observed (fig. 4.2-A). Furthermore, the corresponding -RT melting curve of *MMP9* showed dual-peak suggesting primer-dimer interaction, which suggested the absence of any other amplicons to which the primers can bind. Additionally, gel electrophoresis of PCR products were investigated to check further specificty of the primers in the succinate stimulated genes of interest, as illustrated in figure 4.3. All the genes were below 500 bp. Diffused and smudgy bands suggest the presence of primer-dimer interaction, different isoforms, or multiple transcripts. Apart from *MMP9* gene, all other genes were found to be of low base-pair. The endogenous controls *ACTB* and *TBP* generated multiple bands, which questions the specificity of the genes. Comparing to them, *18S* and *GAPDH* bands were better, and the *18S* band was specific but not as strong as the others. *TNF-α* and *IL-1β* bands were more specific comparing to *MMP9* and *TGF- β1*. The PCR products were not as clean as expected after melting curves analysis and optimization of the PCR settings is required.

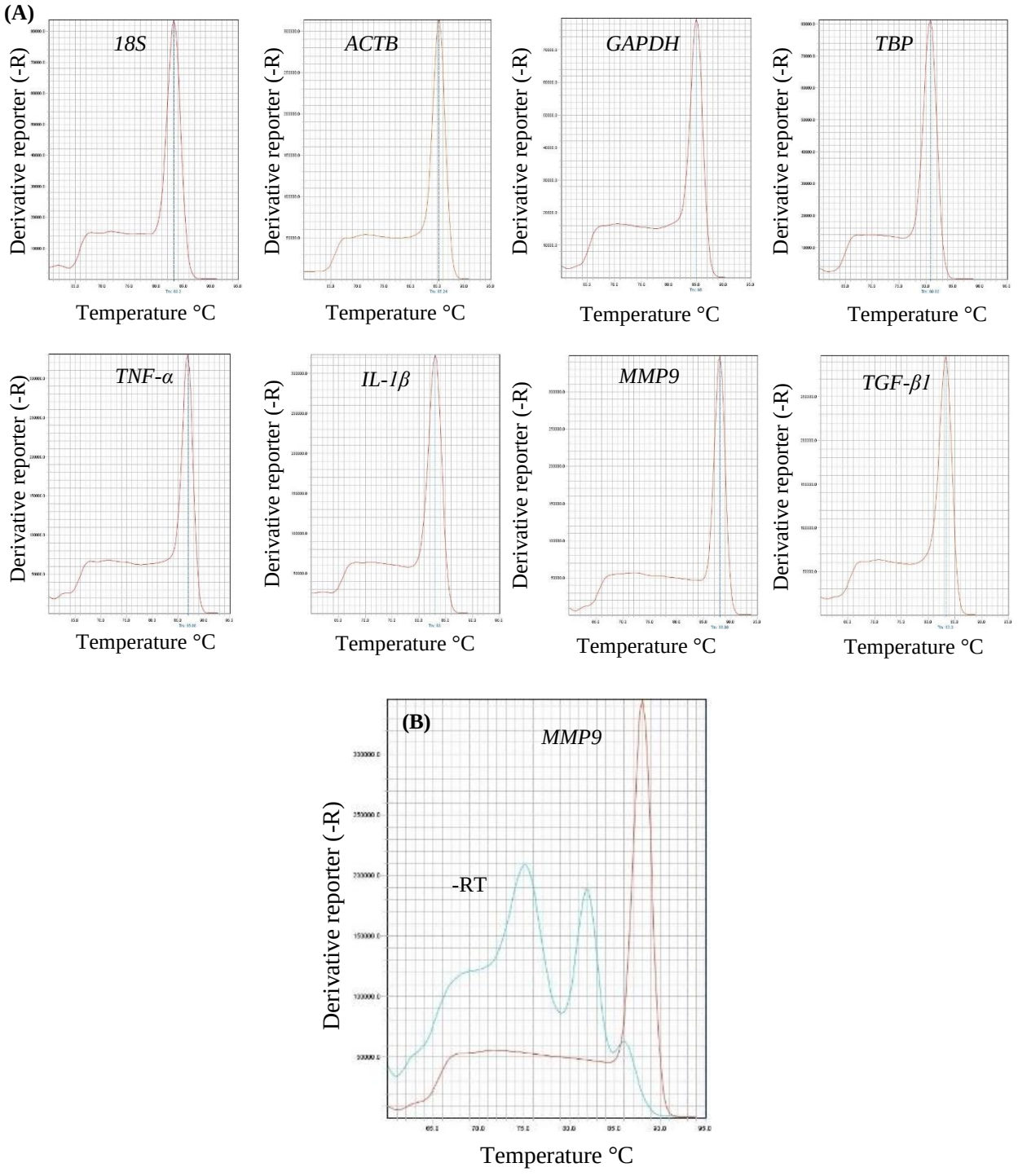


**Figure 4.2: RT-qPCR melting cuve analysis of target genes.**

(A) Melting curve plot of *18S*, *ACTB*, *GAPDH*, *TBP*, *TNF-α*, *IL-1β*, *MMP9*, and *TGF-β1* genes, (B) Melting curve plot of negative control (-RT) and *MMP9*.

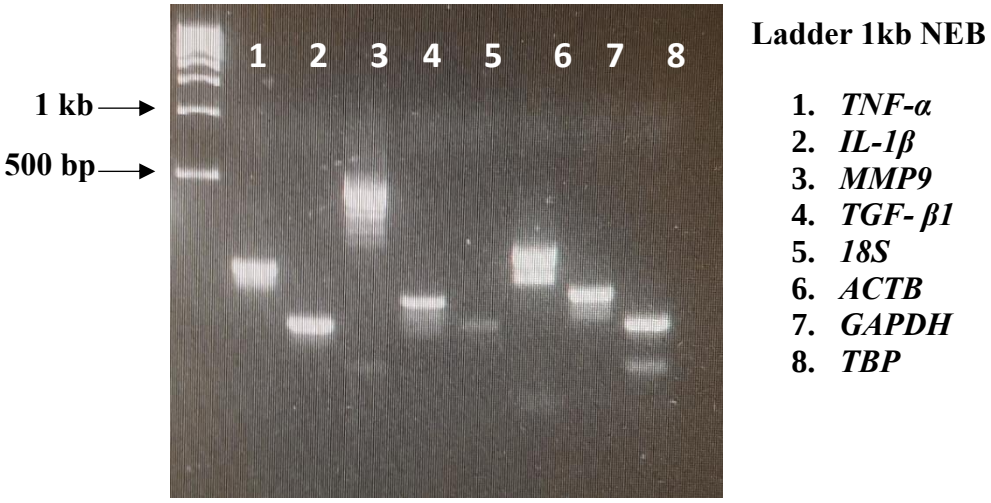


**Figure 4.3: Gel electrophoresis of PCR products.**

### 4.4. *18S* and *GAPDH* genes serve as endogenous controls for THP-1 cells perturbed with succinate

Since it was confirmed that succinate activates the MyD88-dependent TLR4 signaling pathway, the inflammatory activity of all conditions required investigation, which was performed by studying inflammatory cytokine production. For this purpose, the mRNA expression level of released cytokines were investigated by RT-qPCR, and this required selecting endogenous controls. However, from the gel electrophoresis of endogenous controls, it was assumed that *ACTB* and *TBP* PCR had specificity issues with the primers and that could explain the variation of the expression level across samples.

Calculating the difference between the highest mean $C_T$ value and lowest mean $C_T$ value of the corresponding genes (table 4.1) show a difference above 1 (1.32 and 1.42, respectively) for both *ACTB* and *TBP* genes. For *18S* and *GAPDH* genes, the difference was below 1 (0.81 and 0.92, respectively). One cycle difference means approximately $2^n$ difference in DNA number, where n = number of cycles. And since the fluctuation is very little among the four conditions tested for *18S* and *GAPDH* genes, they are both considered stable for this project and used as endogenous controls to normalize the data.

Geometric mean of *18S* and *GAPDH* genes were calculated using the following equation: $\sqrt{}$ (Mean $C_T$ value of 18S) x (Mean $C_T$ value of GAPDH)

Rq value of all four genes: *TNF-α*, *IL-1β*, *MMP9*, and *TGF-β1*, were obtained by a normalization using the geometric mean of *18S* and *GAPDH*.

**Table 4.1: Report of $C_T$ value mean of target genes from RT-qPCR.**

| | | Mean $C_T$ value of targeted genes | | | | | | | |
|---|---|---|---|---|---|---|---|---|---|
| | | *18S* | *ACTB* | *GAPDH* | *TBP* | *TNF-α* | *IL-1β* | *MMP9* | *TGF-β1* |
| Exp 1 conditions | Ctrl | 10.48 | 17.18 | 19.76 | 25.16 | 26.08 | 20.84 | 22.13 | 19.69 |
| | LPS | 10.66 | 17.61 | 20.36 | 25.37 | 19.17 | 15.84 | 22.16 | 19.89 |
| | Suc | 10.64 | 18.37 | 20.44 | 26.43 | 25.59 | 17.95 | 21.96 | 20.23 |
| | LPS+Suc | 11.30 | 18.63 | 20.69 | 26.51 | 25.35 | 17.32 | 22.61 | 19.96 |
| Exp 2 conditions | Ctrl | 10.46 | 17.26 | 19.67 | 25.13 | 24.90 | 19.73 | 19.79 | 18.74 |
| | LPS | 10.66 | 17.62 | 20.29 | 25.30 | 18.02 | 15.07 | 19.91 | 19.00 |
| | Suc | 10.67 | 18.39 | 20.72 | 26.63 | 24.32 | 16.81 | 19.88 | 19.07 |
| | LPS+Suc | 11.26 | 18.45 | 20.58 | 26.61 | 24.15 | 16.36 | 20.38 | 19.03 |

As illustrated in figure 4.4, the $C_T$ value mean of *18S*, *ACTB*, *GAPDH*, and *TBP* showed early to late amplification of genes. All four genes were amplified prior to 30 cycles corresponding to strong positive reactions due to the abundance of target nucleic acids.

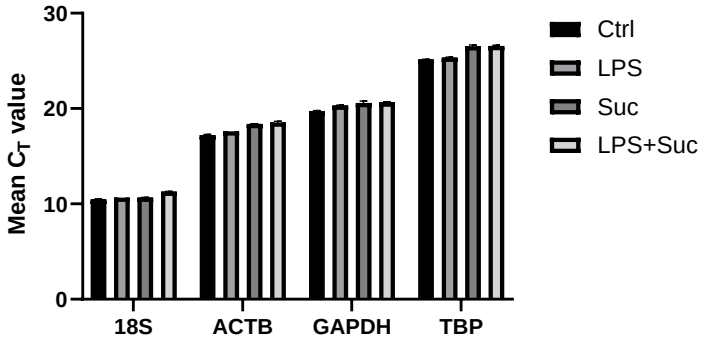


**Figure 4.4: *18S*, *ACTB*, *GAPDH*, and *TBP* gene amplification in the average number of RT-qPCR cycles.**

The experimental data represents technical replicates (n= 2). Error bars represent standard deviation among each gene of interest.

### 4.5. mRNA expression of TLR4 induced cytokines

Four inflammatory cytokines: *TNF-α*, *IL-1β*, *MMP9*, and *TGF-β1*, which are well known to be released upon MyD88-dependent TLR4 signal activation, have been investigated through RT-qPCR.

Figure 4.5 shows normalized mRNA expression levels of *TNF-α*, *IL-1β*, *MMP9*, and *TGF-β1* genes. mRNA expression of *TNF-α* show an increase of 136-fold in LPS treated samples (fig. 4.5 A). *IL-1β* mRNA expression is also increased by 30-fold for LPS treated samples (fig. 4.5 B). Succinate treated samples generated 14-fold increased mRNA expression of *IL-1β* (fig. 4.5 B), while no significant fold change was observed for *TNF-α*. However, when samples were treated with LPS + succinate combination, both mRNA expression of cytokines was decreased significantly. mRNA expression of *TNF*-α was decreased by 130-fold, whereas *IL-1β* mRNA expression was decreased by 6-fold. mRNA expressions of *MMP9* and *TGF-β1* was found to be similar among different conditions (fig. 4.5 C-D).

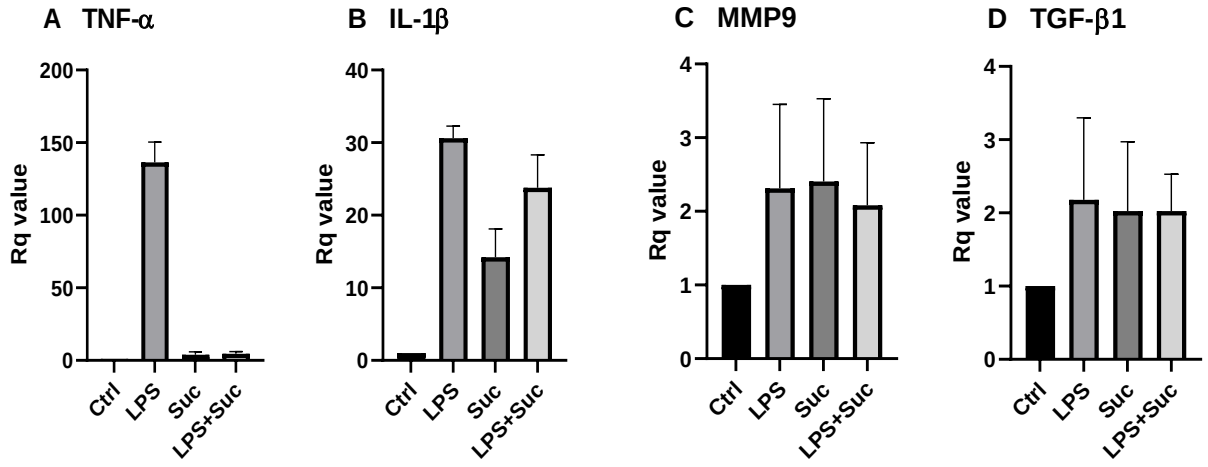


**Figure 4.5: mRNA expression level of *TNF-α*, *IL-1β*, *MMP9*, and *TGF-β1* inflammatory cytokines.**

The plots show the data obtained from 2 biological replicates (n=2) after normalization with the geometric mean of 18S and GAPDH and the control condition. Error bars represent standard deviation within each condition.

# 5. DISCUSSION

The aim of the project was to investigate how succinate, a TCA cycle intermediate metabolite regulates cytokine production through TLR4 signaling pathways in macrophages. For the experiments, THP-1 monocytes were converted to macrophages which were later treated with LPS, succinate, LPS + succinate combination, with a specific dose for five different time points. Protein estimation was performed prior to western blotting, which showed the activated signaling pathways.

Results from total protein estimation suggested that the concentration of TLR4 protein in LPS and succinate combination treated samples were lower than lone LPS and lone succinate treated samples for every time point. From western blot data, succinate was found to be a strong inducer of plasma membrane-bound (MyD88-dependent) TLR4 signaling. But it had no significant effect on endosomal (MyD88-independent) TLR4 pathway. Additionally, the succinate-LPS cross has the capability to dampen the LPS induced TLR4 signaling. These finding has already been established by Mills and colleagues, where they investigated the supportive role of succinate dehydrogenase in inflammatory macrophages[104]. They found that LPS induced IL-1RA and IL-10, two anti-inflammatory cytokines, were inhibited by succinate. The effect of succinate increased early and then depleted later, which was also a finding in this project. Their results suggested that western blotting was performed using p.p65, IκBα, pro-IL-1β proteins, which are activated during the MyD88-dependent TLR4 signaling pathway only. The p.p38MAPK protein expression results from this project coincides with the findings of Mills and colleagues as p.p38MAPK represents the MyD88-dependent TLR4 signaling pathway.

To understand how succinate affects cytokine production through TLR4 signaling pathway, mRNA expression was analyzed using RT-qPCR. For this analysis, optimum endogenous control was required first. From the preliminary background study, four endogenous control were short-listed: *18S*, *ACTB*, *GAPDH*, and *TBP*. *18S* has been used as an endogenous control for gene expression profiling of THP-1 cells infected by *R. prowazekii*[132]. *ACTB* has been established as a consistent reference gene by Microsoft Excel-based applets GeNorm, NormFinder, and BestKeeper housekeeping gene finder softwares[133,134]. In the same vein, *GAPDH* and *TBP* are also well-established endogenous controls[135,136]. Although RT-qPCR melting curve analysis showed amplicon-specific peaks, gel electrophoresis data suggests that both ACTB and TBP had primer

specificity issues. The smudgy and multiple bands are probable results of primer-dimer interaction, activation of multiple isoforms, or presence of multiple transcripts. To solve the primer specificity issue, the RT-qPCR requires optimization. Additionally, the selection of endogenous controls also depends on specific factors such as cell line, condition, etc. The qPCR results for the endogenous control suggested that all four genes could produce strong positive reactions due to the abundance of target nucleic acids. However, using a single reference gene can produce inaccurate expression leading to false-positive results during data normalization[137]. To avoid such anomalies, more than one reference gene was selected. Analysis of the $C_T$ value suggested that the difference of highest and lowest $C_T$ value for *ACTB* and *TBP* are higher than 1.0. *18S* and *GAPDH*, on the other hand, had a much lower difference between the highest and lowest $C_T$ value. Hence, for this project, *18S* and *GAPDH* genes were selected to serve as endogenous controls.

To investigate the mRNA expression level of inflammatory cytokines, four genes: *TNF-α*, *IL-1β*, *MMP9*, and *TGF-β1* were selected. *TNF-α* is one of the key proinflammatory cytokines, which upon activation by TLR4 induction, can associate with two major signaling cascades. One is the apoptotic signaling pathway through TNF receptor 1 (TNFR1), and the other is the inflammatory signaling cascade mediated through TRADD, further recruiting TRAF2 and RIP to the TNFR1 complex[138]. *Interleukin-1β* (*IL-1β*) is also a proinflammatory mediator of inflammation. A well-established signaling pathway for *IL-1β* activation is mediated through adaptors MyD88-IRAK-1[139]. Upon TLR4 activation, matrix metalloproteinase-9 (*MMP-9*) is expressed through p38 and JNK pathway. *MMP9* is then released from the nucleus as *pro-MMP9* in the cytoplasm from *AP-1-MMP9* gene complex[140]. Similarly, *TGF-β1* is also expressed through the MAPK-NF-κB pathway[130].

RT-qPCR results showed that LPS treated samples produced very high (136-fold) *TNF-α* mRNA expression compared to unstimulated control samples, which aligns with previous findings[39]. On the contrary, succinate treated samples did not show any increase in *TNF-α* mRNA expression[39]. For LPS and succinate combination treated samples, succinate has been found to greatly reduce LPS induced *TNF-α* mRNA expression[127].

LPS treated samples also produced a high level of *IL-1β* mRNA expression. Again, when treated with LPS and succinate combination, LPS induced high mRNA expression of *IL-1β* was dampened by succinate (From 30-fold to 24-fold). Furthermore, when compared to succinate alone, treatment

with LPS and succinate combination increases *IL-1β* mRNA expression (from 14-fold to 24-fold), similar to the finding of Tannahill and colleagues[96]. Their study also showed that *IL-1β* mRNA was expressed higher in lone LPS treated samples comparing to lone succinate treated samples which is also confirmed by the present finding.

*MMP9* mRNA expression was found to be very low comparing to *TNF-α* and *IL-1β* mRNA expression. *MMP9* gene expression requires MyD88-dependent TLR4 signaling and NF-κB activation[141]. RT-qPCR result suggests that there is no significant difference in *MMP9* mRNA expression between LPS, succinate, and LPS and succinate combination induced TLR4 activation. Although succinate has been found to be associated with *MMP9* mRNA expression, association of LPS and succinate combination, and MMP9 has yet to be studied extensively[142].

Similar to *MMP9*, the *TGF-β1* mRNA expression level was very low. Furthermore, there was no significant difference in *TGF-β1* mRNA expression among the different conditions. This can be justified by the involved signaling mechanism. *TGF-β1* activates the SMAD3 (SMAD Family Member 3), which eventually activates the SMAD3-target gene SMAD6 (SMAD Family Member 6). SMAD3 and SMAD6 are the main signal transducers for *TGF-β1*. Upon activation, SMAD6 inhibits LPS-induced NF-κB activation. LPS then overrides the SMAD3 activation by phosphorylation through TLR4–IRAK1-activated ERK1/2. As SMAD3 is inhibited, so is the *TGF-β1* mRNA expression[143]. Since succinate can also activate NF-κB through TLR4 signaling, a similar inhibitory mechanism is also applicable for succinate.

Overall results from this project suggest that disodium succinate has inflammatory effects, while it can also crosstalk with LPS and possibly regulate the inflammatory effects of LPS. Similar contradictory results have been established by various other studies as well[96,104-106,130]. Both diethyl succinate and disodium succinate have been investigated throughout these studies. Tannahill and colleagues investigated the effect of diethyl succinate on inflammatory signaling in mBMDMs and found that succinate induced HIF-1α protein expression and subsequent *IL-1β* inflammatory cytokine production. Furthermore, cell surface receptor SUCNR1 was found to induce *IL-1β* secretion due to the affinity of succinate towards membrane-bound receptors. Based on similar experimental settings from Tannahill and colleagues, and Harber and colleagues investigated the similar effect of diethyl succinate and found contradictory results[130]. The results suggested that diethyl succinate reduces the secretion of the inflammatory mediator, *IL-6*, in mBMDMs. Harber

and colleagues then investigated disodium succinate, which suggested that disodium succinate mediated the anti-inflammatory response of *IFN-γ* through a SUCNR1-independent mechanism in mBMDMs[130]. Additionally, disodium succinate has also been found to mediate the anti-inflammatory effect of *PPARγ* and *MRC1* through the SUCNR1-dependent mechanism in mBMDMs[105,106]. The SUCNR1-dependency was justified by Kieran and colleagues, as they claimed that a significantly high expression of SUCNR1 was observed in mBMDMs comparing to other cell lines[105].

Findings from the current project suggest that disodium succinate showed inflammation-modulating potential by producing inflammatory cytokines. At the same time, disodium succinate has shown scope for LPS-disodium succinate crosstalk, leading to possible inflammation regulatory activity by dampening inflammatory cytokine production. Although disodium succinate has been well established for mediating anti-inflammatory response, the inflammation regulatory response requires more in-depth investigation.

# 6. LIMITATIONS

The study was conducted on THP-1 macrophages only. Also, only one TLR ligand, TLR4, was experimented on. Due to time constraints, ELISA and cytotoxicity assay was not performed, which would have provided insight about protein quantification and cell-mediated as well as chemical-mediated cytotoxicity, respectively. For the same reason, more technical and biological replicates could not be studied, and optimization of RT-qPCR could not be performed.

Activation of SUCNR1 can, however, activate the MAPK pathway. Since disodium succinate can activate the SUCNR1 receptor, hypothetically justifies the results from this project; (i) Disodium produces inflammatory cytokines through the SUCNR1-dependent mechanism, (ii) the inflammation regulatory mechanism of disodium succinate can be SUCNR1-dependent. However, the experimental setting did not include any KO-SUCNR1 samples, it cannot be suggested for sure whether the inflammatory regulation of disodium succinate is mediated through SUCNR1-dependent or -independent mechanism.

Considering the fact that the LPS and disodium succinate concentration along with the stimulation times for this project were similar to the ones mentioned earlier, it can only be assumed that differences in the culture methods such as cell line (THP-1 vs. mBMDM vs. Myeloid cell-specific KO-Sucnr1 mice), medium (RPMI-1640 vs. DMEM) or fetal serum (FCS vs. FBS), could have resulted in these differences in response to succinate. And similar concern has been previously suggested as well[130].

## 7. CONCLUSION

This project was aimed to understand how succinate affects the inflammatory signaling through the TLR-4 signaling pathway. Disodium succinate being the component of interest, provided contradictory results, which was expected from the background study as well. The finding of disodium succinate to be an inflammation inducer, contradicts the established results from various previous studies in different experimental settings. Similarly, the regulatory effect of disodium succinate over LPS induced inflammation requires further investigation. Understanding the SUCNR1-disodium succinate axis mechanism can later be applied to diseased conditions, which display altered local or systemic levels of disodium succinate. Rheumatoid arthritis is one such condition where high succinate levels can be observed in the synovium fluid of patients[144]. By observing the inflammatory regulation mechanisms of disodium succinate as well as its analogs and prodrugs, appropriate treatment procedures can be developed for such diseases. Since these finds are contradictory to many initial articles, a lot of questions arise on how disodium succinate exactly regulates inflammation in macrophages. This data, in combination with results from previous studies, indicate how complex the field of immunometabolism is and how one molecule can play diverse roles in modulating polar opposite effects.

## 8. FUTURE PLANS

1. Perform more studies with succinate to confirm our findings regarding inflammatory regulation.
2. Study the SUCNR1-disodium succinate axis mechanism to understand the inflammation regulation.
3. Study with specific signaling mechanism of disodium succinate induced TLR4 and find out which signaling porting is altered.
4. Study disodium succinate prodrugs in the same experimental settings.

# 9. REFERENCES


1 Foligne, B. *et al.* Correlation between in vitro and in vivo immunomodulatory properties of lactic acid bacteria. *World journal of gastroenterology: WJG* **13**, 236 (2007).

2 Tsuchiya, S. *et al.* Establishment and characterization of a human acute monocytic leukemia cell line (THP-1). *Int J Cancer* **26**, 171-176, doi:10.1002/ijc.2910260208 (1980).

3 Daigneault, M., Preston, J. A., Marriott, H. M., Whyte, M. K. & Dockrell, D. H. The identification of markers of macrophage differentiation in PMA-stimulated THP-1 cells and monocyte-derived macrophages. *PloS one* **5**, e8668 (2010).

4 Cousins, R. J. *et al.* A global view of the selectivity of zinc deprivation and excess on genes expressed in human THP-1 mononuclear cells. *Proceedings of the National Academy of Sciences* **100**, 6952-6957 (2003).

5 Baum, L. L. Role of humoral immunity in host defense against HIV. *Current HIV/AIDS Reports* **7**, 11-18 (2010).

6 Elgueta, R., De Vries, V. C. & Noelle, R. J. The immortality of humoral immunity. *Immunological reviews* **236**, 139-150 (2010).

7 Vesely, M. D., Kershaw, M. H., Schreiber, R. D. & Smyth, M. J. Natural innate and adaptive immunity to cancer. *Annual review of immunology* **29**, 235-271 (2011).

8 Dranoff, G. Cytokines in cancer pathogenesis and cancer therapy. *Nature Reviews Cancer* **4**, 11-22 (2004).

9 Borriello, F., Zanoni, I. & Granucci, F. Cellular and molecular mechanisms of antifungal innate immunity at epithelial barriers: The role of C-type lectin receptors. *European journal of immunology* **50**, 317-325 (2020).

10 Bos, J., De Rie, M., Teunissen, M. & Piskin, G. Psoriasis: dysregulation of innate immunity. *British Journal of Dermatology* **152**, 1098-1107 (2005).

11 Kumar, H., Kawai, T. & Akira, S. Pathogen recognition in the innate immune response. *Biochemical Journal* **420**, 1-16 (2009).

12 Si-Tahar, M., Touqui, L. & Chignard, M. Innate immunity and inflammation–two facets of the same anti-infectious reaction. *Clinical & Experimental Immunology* **156**, 194-198 (2009).

13 Broz, P. & Dixit, V. M. Inflammasomes: mechanism of assembly, regulation and signalling. *Nature Reviews Immunology* **16**, 407-420, doi:10.1038/nri.2016.58 (2016).

14 Martinon, F., Burns, K. & Tschopp, J. The Inflammasome: A Molecular Platform Triggering Activation of Inflammatory Caspases and Processing of proIL-&#x3b2. *Molecular Cell* **10**, 417-426, doi:10.1016/S1097-2765(02)00599-3 (2002).

15 Winsor, N., Krustev, C., Bruce, J., Philpott, D. J. & Girardin, S. E. Canonical and noncanonical inflammasomes in intestinal epithelial cells. *Cellular Microbiology* **21**, e13079, doi:https://doi.org/10.1111/cmi.13079 (2019).

16 Wang, Q. *et al.* Ghrelin protects the heart against ischemia/reperfusion injury via inhibition of TLR4/NLRP3 inflammasome pathway. *Life sciences* **186**, 50-58 (2017).

17 Su, Q. *et al.* Effects of the TLR4/Myd88/NF-κB signaling pathway on NLRP3 inflammasome in coronary microembolization-induced myocardial injury. *Cellular Physiology and Biochemistry* **47**, 1497-1508 (2018).

18 Zhang, A. *et al.* Mechanisms that lead to the regulation of NLRP3 inflammasome expression and activation in human dental pulp fibroblasts. *Molecular Immunology* **66**, 253-262, doi:https://doi.org/10.1016/j.molimm.2015.03.009 (2015).

19 Zhang, X. *et al.* The protective effect of Luteolin on myocardial ischemia/reperfusion (I/R) injury through TLR4/NF-κB/NLRP3 inflammasome pathway. *Biomedicine & Pharmacotherapy* **91**, 1042-1052 (2017).

20 Anderson, K. V., Jürgens, G. & Nüsslein-Volhard, C. Establishment of dorsal-ventral polarity in the Drosophila embryo: genetic studies on the role of the Toll gene product. *Cell* **42**, 779-789 (1985).

21 Cherry, S. & Silverman, N. Host-pathogen interactions in drosophila: new tricks from an old friend. *Nature immunology* **7**, 911-917 (2006).
22 Medzhitov, R., Preston-Hurlburt, P. & Janeway, C. A. A human homologue of the Drosophila Toll protein signals activation of adaptive immunity. *Nature* **388**, 394-397 (1997).
23 Akira, S., Uematsu, S. & Takeuchi, O. Pathogen recognition and innate immunity. *Cell* **124**, 783-801 (2006).
24 Lee, H. K. & Iwasaki, A. in *Seminars in immunology*. 48-55 (Elsevier).
25 Matsushima, N. *et al.* Comparative sequence analysis of leucine-rich repeats (LRRs) within vertebrate toll-like receptors. *BMC genomics* **8**, 1-20 (2007).
26 Jang, T.-h. & Park, H. H. Crystal Structure of TIR Domain of TLR6 Reveals Novel Dimeric Interface of TIR–TIR Interaction for Toll-Like Receptor Signaling Pathway. *Journal of Molecular Biology* **426**, 3305-3313, doi:https://doi.org/10.1016/j.jmb.2014.07.024 (2014).
27 Gao, W., Xiong, Y., Li, Q. & Yang, H. Inhibition of toll-like receptor signaling as a promising therapy for inflammatory diseases: a journey from molecular to nano therapeutics. *Frontiers in physiology* **8**, 508 (2017).
28 O'Neill, L. A. & Bowie, A. G. The family of five: TIR-domain-containing adaptors in Toll-like receptor signalling. *Nature Reviews Immunology* **7**, 353-364 (2007).
29 Pendergraft, W. F. & Means, T. K. in *Systemic Lupus Erythematosus* (ed George C. Tsokos) 143-151 (Academic Press, 2016).
30 Kawai, T. & Akira, S. TLR signaling. *Cell Death Differ* **13**, 816-825, doi:10.1038/sj.cdd.4401850 (2006).
31 Yu, L., Wang, L. & Chen, S. Endogenous toll-like receptor ligands and their biological significance. *Journal of cellular and molecular medicine* **14**, 2592-2603 (2010).
32 Jiménez-Dalmaroni, M. J., Gerswhin, M. E. & Adamopoulos, I. E. The critical role of toll-like receptors—from microbial recognition to autoimmunity: a comprehensive review. *Autoimmunity reviews* **15**, 1-8 (2016).
33 Goulopoulou, S., McCarthy, C. G. & Webb, R. C. Toll-like receptors in the vascular system: sensing the dangers within. *Pharmacological reviews* **68**, 142-167 (2016).
34 Rock, F. L., Hardiman, G., Timans, J. C., Kastelein, R. A. & Bazan, J. F. A family of human receptors structurally related to Drosophila Toll. *Proceedings of the National Academy of Sciences* **95**, 588-593 (1998).
35 Muzio, M. *et al.* Differential expression and regulation of toll-like receptors (TLR) in human leukocytes: selective expression of TLR3 in dendritic cells. *The Journal of Immunology* **164**, 5998-6004 (2000).
36 Kikuchi, T. *et al.* Gene expression of osteoclast differentiation factor is induced by lipopolysaccharide in mouse osteoblasts via Toll-like receptors. *The Journal of Immunology* **166**, 3574-3579 (2001).
37 Frantz, S. *et al.* Toll4 (TLR4) expression in cardiac myocytes in normal and failing myocardium. *The Journal of clinical investigation* **104**, 271-280 (1999).
38 Vaure, C. & Liu, Y. A Comparative Review of Toll-Like Receptor 4 Expression and Functionality in Different Animal Species. *Frontiers in Immunology* **5**, doi:10.3389/fimmu.2014.00316 (2014).
39 Lu, Y.-C., Yeh, W.-C. & Ohashi, P. S. LPS/TLR4 signal transduction pathway. *Cytokine* **42**, 145-151 (2008).
40 Gohda, J., Matsumura, T. & Inoue, J.-i. Cutting edge: TNFR-associated factor (TRAF) 6 is essential for MyD88-dependent pathway but not Toll/IL-1 receptor domain-containing adaptor-inducing IFN-β (TRIF)-dependent pathway in TLR signaling. *The Journal of Immunology* **173**, 2913-2917 (2004).
41 Lomaga, M. A. *et al.* TRAF6 deficiency results in osteopetrosis and defective interleukin-1, CD40, and LPS signaling. *Genes & development* **13**, 1015-1024 (1999).

42 Pålsson-McDermott, E. M. & O'Neill, L. A. J. Signal transduction by the lipopolysaccharide receptor, Toll-like receptor-4. *Immunology* **113**, 153-162, doi:https://doi.org/10.1111/j.1365-2567.2004.01976.x (2004).
43 Beutler, B. & Rietschel, E. T. Innate immune sensing and its roots: the story of endotoxin. *Nature Reviews Immunology* **3**, 169-176 (2003).
44 Raetz, C. R. & Whitfield, C. Lipopolysaccharide endotoxins. *Annual review of biochemistry* **71**, 635-700 (2002).
45 Miller, S. I., Ernst, R. K. & Bader, M. W. LPS, TLR4 and infectious disease diversity. *Nature Reviews Microbiology* **3**, 36-46 (2005).
46 Netea, M. G., van Deuren, M., Kullberg, B. J., Cavaillon, J. M. & Van der Meer, J. W. Does the shape of lipid A determine the interaction of LPS with Toll-like receptors? *Trends Immunol* **23**, 135-139, doi:10.1016/s1471-4906(01)02169-x (2002).
47 Gioannini, T. L. & Weiss, J. P. Regulation of interactions of Gram-negative bacterial endotoxins with mammalian cells. *Immunologic research* **39**, 249-260 (2007).
48 Hailman, E. *et al.* Lipopolysaccharide (LPS)-binding protein accelerates the binding of LPS to CD14. *Journal of Experimental Medicine* **179**, 269-277 (1994).
49 Tobias, P. S., Soldau, K., Gegner, J. A., Mintz, D. & Ulevitch, R. J. Lipopolysaccharide binding protein-mediated complexation of lipopolysaccharide with soluble CD14. *Journal of Biological Chemistry* **270**, 10482-10488 (1995).
50 Ferrero, E. & Goyert, S. M. Nucleotide sequence of the gene encoding the monocyte differentiation antigen, CD14. *Nucleic acids research* **16**, 4173 (1988).
51 Haziot, A. *et al.* The monocyte differentiation antigen, CD14, is anchored to the cell membrane by a phosphatidylinositol linkage. *The Journal of Immunology* **141**, 547-552 (1988).
52 Poltorak, A. *et al.* Defective LPS signaling in C3H/HeJ and C57BL/10ScCr mice: mutations in Tlr4 gene. *Science* **282**, 2085-2088 (1998).
53 Schromm, A. B. *et al.* Molecular genetic analysis of an endotoxin nonresponder mutant cell line: a point mutation in a conserved region of MD-2 abolishes endotoxin-induced signaling. *The Journal of experimental medicine* **194**, 79-88 (2001).
54 Laskin, D. L. Macrophages and inflammatory mediators in chemical toxicity: a battle of forces. *Chemical research in toxicology* **22**, 1376-1385 (2009).
55 Tada, H. *et al.* Saccharomyces cerevisiae-and Candida albicans-derived mannan induced production of tumor necrosis factor alpha by human monocytes in a CD14-and Toll-like receptor 4-dependent manner. *Microbiology and immunology* **46**, 503-512 (2002).
56 Ziegler-Heitbrock, L. The CD14+ CD16+ blood monocytes: their role in infection and inflammation. *Journal of leukocyte biology* **81**, 584-592 (2007).
57 Poole, J. A. *et al.* Repetitive organic dust exposure in vitro impairs macrophage differentiation and function. *Journal of allergy and clinical immunology* **122**, 375-382. e374 (2008).
58 Fujiwara, N. & Kobayashi, K. Macrophages in inflammation. *Current Drug Targets-Inflammation & Allergy* **4**, 281-286 (2005).
59 Galli, S. J., Borregaard, N. & Wynn, T. A. Phenotypic and functional plasticity of cells of innate immunity: macrophages, mast cells and neutrophils. *Nature immunology* **12**, 1035 (2011).
60 Lea, T. Immunologi og immunologiske teknikker (Vol. 3). *Bergen: Fagbokforlaget Vigmostad & Bjørke AS* (2006).
61 Vega, M. & Corbi, A. Human macrophage activation: too many functions and phenotypes for a single cell type. *Immunologia* **25**, 248-272 (2006).
62 Taylor, P. R. *et al.* Macrophage receptors and immune recognition. *Annu. Rev. Immunol.* **23**, 901-944 (2005).
63 Patel, U. *et al.* Macrophage polarization in response to epigenetic modifiers during infection and inflammation. *Drug discovery today* **22**, 186-193 (2017).
64 Mantovani, A. *et al.* The chemokine system in diverse forms of macrophage activation and polarization. *Trends in immunology* **25**, 677-686 (2004).

65 Canton, J. Phagosome maturation in polarized macrophages. *Journal of leukocyte biology* **96**, 729-738 (2014).
66 Gordon, S. Alternative activation of macrophages. *Nature reviews immunology* **3**, 23-35 (2003).
67 Mosser, D. M. & Edwards, J. P. Exploring the full spectrum of macrophage activation. *Nature reviews immunology* **8**, 958-969 (2008).
68 Lampiasi, N., Russo, R. & Zito, F. The alternative faces of macrophage generate osteoclasts. *BioMed research international* **2016** (2016).
69 Atri, C., Guerfali, F. Z. & Laouini, D. Role of human macrophage polarization in inflammation during infectious diseases. *International journal of molecular sciences* **19**, 1801 (2018).
70 Yao, Y., Xu, X.-H. & Jin, L. Macrophage Polarization in Physiological and Pathological Pregnancy. *Frontiers in Immunology* **10**, 792 (2019).
71 Martinez, F. O., Helming, L. & Gordon, S. Alternative activation of macrophages: an immunologic functional perspective. *Annual review of immunology* **27**, 451-483 (2009).
72 Murray, P. J. Macrophage polarization. *Annual review of physiology* **79**, 541-566 (2017).
73 Weisser, S. B., McLarren, K. W., Kuroda, E. & Sly, L. M. in *Basic Cell Culture Protocols* 225-239 (Springer, 2013).
74 Martinez, F. O. & Gordon, S. The M1 and M2 paradigm of macrophage activation: time for reassessment. *F1000prime reports* **6** (2014).
75 Porta, C., Riboldi, E., Ippolito, A. & Sica, A. 4 edn 237-248 (Elsevier).
76 Wang, N., Liang, H. & Zen, K. Molecular mechanisms that influence the macrophage M1–M2 polarization balance. *Frontiers in immunology* **5**, 614 (2014).
77 O'Shea, J. J. & Paul, W. E. Mechanisms underlying lineage commitment and plasticity of helper CD4+ T cells. *Science* **327**, 1098-1102 (2010).
78 Ferrante, C. J. *et al.* The adenosine-dependent angiogenic switch of macrophages to an M2-like phenotype is independent of interleukin-4 receptor alpha (IL-4Rα) signaling. *Inflammation* **36**, 921-931 (2013).
79 Mantovani, A., Biswas, S. K., Galdiero, M. R., Sica, A. & Locati, M. Macrophage plasticity and polarization in tissue repair and remodelling. *The Journal of pathology* **229**, 176-185 (2013).
80 Wang, Y. *et al.* Macrophage-derived extracellular vesicles: diverse mediators of pathology and therapeutics in multiple diseases. *Cell Death & Disease* **11**, 924, doi:10.1038/s41419-020-03127-z (2020).
81 Auwerx, J. The human leukemia cell line, THP-1: A multifacetted model for the study of monocyte-macrophage differentiation. *Experientia* **47**, 22-31, doi:10.1007/BF02041244 (1991).
82 Park, E. K. *et al.* Optimized THP-1 differentiation is required for the detection of responses to weak stimuli. *Inflamm Res* **56**, 45-50, doi:10.1007/s00011-007-6115-5 (2007).
83 Auwerx, J., Staels, B., Van Vaeck, E., Verhoeven, G. & Ceuppens, J. (THP-1, 1990).
84 Zuckerman, S. H. & Schreiber, R. D. Up-Regulation of Gamma Interferon Receptors on the Human Monocytic Cell Line U937 by 1, 25-Dihydroxyvitamin D3 and Granulocyte-Macrophage Colony Stimulating Factor. *Journal of leukocyte biology* **44**, 187-191 (1988).
85 Gordon, S. & Taylor, P. R. Monocyte and macrophage heterogeneity. *Nature reviews immunology* **5**, 953-964 (2005).
86 Pinto, S. M. *et al.* Dose-dependent phorbol 12-myristate-13-acetate-mediated monocyte-to-macrophage differentiation induces unique proteomic signatures in THP-1 cells. *bioRxiv*, 2020.2002.2027.968016, doi:10.1101/2020.02.27.968016 (2020).
87 Hotamisligil, G. S. Foundations of immunometabolism and implications for metabolic health and disease. *Immunity* **47**, 406-420 (2017).
88 Andrejeva, G. & Rathmell, J. C. Similarities and distinctions of cancer and immune metabolism in inflammation and tumors. *Cell metabolism* **26**, 49-70 (2017).
89 Tretter, L., Patocs, A. & Chinopoulos, C. Succinate, an intermediate in metabolism, signal transduction, ROS, hypoxia, and tumorigenesis. *Biochimica et Biophysica Acta (BBA) - Bioenergetics* **1857**, 1086-1101, doi:https://doi.org/10.1016/j.bbabio.2016.03.012 (2016).

90 Mills, E. & O'Neill, L. A. Succinate: a metabolic signal in inflammation. *Trends Cell Biol* **24**, 313-320, doi:10.1016/j.tcb.2013.11.008 (2014).
91 Yang, M., Soga, T. & Pollard, P. J. Oncometabolites: linking altered metabolism with cancer. *J Clin Invest* **123**, 3652-3658, doi:10.1172/jci67228 (2013).
92 Chouchani, E. T. *et al.* Ischaemic accumulation of succinate controls reperfusion injury through mitochondrial ROS. *Nature* **515**, 431-435, doi:10.1038/nature13909 (2014).
93 Fernie, A. R., Carrari, F. & Sweetlove, L. J. Respiratory metabolism: glycolysis, the TCA cycle and mitochondrial electron transport. *Current Opinion in Plant Biology* **7**, 254-261, doi:https://doi.org/10.1016/j.pbi.2004.03.007 (2004).
94 Murphy, M. P. & O'Neill, L. A. J. Krebs Cycle Reimagined: The Emerging Roles of Succinate and Itaconate as Signal Transducers. *Cell* **174**, 780-784, doi:10.1016/j.cell.2018.07.030 (2018).
95 Jha, A. K. *et al.* Network integration of parallel metabolic and transcriptional data reveals metabolic modules that regulate macrophage polarization. *Immunity* **42**, 419-430, doi:10.1016/j.immuni.2015.02.005 (2015).
96 Tannahill, G. M. *et al.* Succinate is an inflammatory signal that induces IL-1β through HIF-1α. *Nature* **496**, 238-242, doi:10.1038/nature11986 (2013).
97 Kietzmann, T. & Görlach, A. Reactive oxygen species in the control of hypoxia-inducible factor-mediated gene expression. *Seminars in Cell & Developmental Biology* **16**, 474-486, doi:https://doi.org/10.1016/j.semcdb.2005.03.010 (2005).
98 Guzy, R. D., Sharma, B., Bell, E., Chandel, N. S. & Schumacker, P. T. Loss of the SdhB, but Not the SdhA, subunit of complex II triggers reactive oxygen species-dependent hypoxia-inducible factor activation and tumorigenesis. *Mol Cell Biol* **28**, 718-731, doi:10.1128/mcb.01338-07 (2008).
99 Gilissen, J., Jouret, F., Pirotte, B. & Hanson, J. Insight into SUCNR1 (GPR91) structure and function. *Pharmacology & Therapeutics* **159**, 56-65, doi:https://doi.org/10.1016/j.pharmthera.2016.01.008 (2016).
100 Rubic, T. *et al.* Triggering the succinate receptor GPR91 on dendritic cells enhances immunity. *Nature Immunology* **9**, 1261-1269, doi:10.1038/ni.1657 (2008).
101 de Castro Fonseca, M., Aguiar, C. J., da Rocha Franco, J. A., Gingold, R. N. & Leite, M. F. GPR91: expanding the frontiers of Krebs cycle intermediates. *Cell Communication and Signaling* **14**, 3, doi:10.1186/s12964-016-0126-1 (2016).
102 Palsson-McDermott, E. M. & O'Neill, L. A. The Warburg effect then and now: from cancer to inflammatory diseases. *Bioessays* **35**, 965-973, doi:10.1002/bies.201300084 (2013).
103 Otto, A. M. Warburg effect(s)-a biographical sketch of Otto Warburg and his impacts on tumor metabolism. *Cancer Metab* **4**, 5-5, doi:10.1186/s40170-016-0145-9 (2016).
104 Mills, E. L. *et al.* Succinate Dehydrogenase Supports Metabolic Repurposing of Mitochondria to Drive Inflammatory Macrophages. *Cell* **167**, 457-470.e413, doi:10.1016/j.cell.2016.08.064 (2016).
105 Keiran, N. *et al.* SUCNR1 controls an anti-inflammatory program in macrophages to regulate the metabolic response to obesity. *Nature Immunology* **20**, 581-592, doi:10.1038/s41590-019-0372-7 (2019).
106 Wu, J. Y. *et al.* Cancer-Derived Succinate Promotes Macrophage Polarization and Cancer Metastasis via Succinate Receptor. *Mol Cell* **77**, 213-227.e215, doi:10.1016/j.molcel.2019.10.023 (2020).
107 Inc, B. C. *BECKMAN COULTER® Z Series User Manual 9914591-D*, <https://fccf.sitehost.iu.edu/pdf/Z2Manual.pdf> (1992-2002).
108 Schwende, H., Fitzke, E., Ambs, P. & Dieter, P. Differences in the state of differentiation of THP-1 cells induced by phorbol ester and 1, 25-dihydroxyvitamin D3. *Journal of leukocyte biology* **59**, 555-561 (1996).
109 Mosser, D. M. & Zhang, X. Activation of murine macrophages. *Curr Protoc Immunol* **Chapter 14**, Unit 14.12, doi:10.1002/0471142735.im1402s83 (2008).

110 Tang, C. B. *et al.* Identification of Rosmarinic Acid-Adducted Sites in Meat Proteins in a Gel Model under Oxidative Stress by Triple TOF MS/MS. *J Agric Food Chem* **64**, 6466-6476, doi:10.1021/acs.jafc.6b02438 (2016).
111 Alonso-Orgaz, S. *et al.* Differential protein expression analysis of degenerative aortic stenosis by iTRAQ labeling. *Methods Mol Biol* **1005**, 109-117, doi:10.1007/978-1-62703-386-2_9 (2013).
112 SCIENTIFIC, T. *Pierce™ BCA Protein Assay Kit User guide*, <https://www.thermofisher.com/document-connect/document-connect.html?url=https://assets.thermofisher.com/TFS-Assets/LSG/manuals/MAN0011430_Pierce_BCA_Protein_Asy_UG.pdf> (2020).
113 Smith, P. K. *et al.* Measurement of protein using bicinchoninic acid. *Anal Biochem* **150**, 76-85, doi:10.1016/0003-2697(85)90442-7 (1985).
114 Bio-Rad Laboratories, I. *iMark™ Microplate Absorbance Reader Instruction Manual* <https://www.bio-rad.com/webroot/web/pdf/lsr/literature/10013301i.pdf> (
115 Mahmood, T. & Yang, P. C. Western blot: technique, theory, and trouble shooting. *N Am J Med Sci* **4**, 429-434, doi:10.4103/1947-2714.100998 (2012).
116 Invitrogen™. *NuPAGE® Technical Guide*, <https://www.thermofisher.com/document-connect/document-connect.html?url=https://assets.thermofisher.com/TFS-Assets/LSG/manuals/nupage_tech_man.pdf> (2010).
117 Invitrogen™. *SeeBlue® Plus2 Pre-Stained Protein Standard*, <https://www.thermofisher.com/document-connect/document-connect.html?url=https://assets.thermofisher.com/TFS-Assets/LSG/manuals/SeeBluePlus2PreStainedStnd_man.pdf> (2014).
118 Invitrogen™. *MagicMark™ XP Western Protein Standard*, <https://www.thermofisher.com/document-connect/document-connect.html?url=https://assets.thermofisher.com/TFS-Assets/LSG/manuals/MagicMarkXPWesternProteinStnd_man.pdf> (2014).
119 Invitrogen™. *Protein gel electrophoresis technical handbook*, <https://www.thermofisher.com/document-connect/document-connect.html?url=https://assets.thermofisher.com/TFS-Assets/BID/Handbooks/protein-gel-electrophoresis-technical-handbook.pdf> (2016).
120 Biologicals, N. *Western blot membrane stripping for reprobing*, <https://www.novusbio.com/support/support-by-application/stripping-for-reprobing> (2021).
121 Scientific™, T. *SuperSignal West Femto Maximum Sensitivity Substrate*, <https://assets.thermofisher.com/TFS-Assets/LSG/manuals/MAN0011345_SupSig_West_Femto_MaxSensi_Subs_UG.pdf> (2014).
122 QIAGEN. *RNeasy® Mini Handbook*, 2019).
123 SCIENTIFIC, T. *High-Capacity RNA-to-cDNA™ Kit Product information sheet*, <https://www.thermofisher.com/document-connect/document-connect.html?url=https://assets.thermofisher.com/TFS-Assets/LSG/manuals/4387949_RNAtocDNA_PI.pdf> (2018).
124 Rychlik, W., Spencer, W. J. & Rhoads, R. E. Optimization of the annealing temperature for DNA amplification in vitro. *Nucleic Acids Research* **18**, 6409-6412, doi:10.1093/nar/18.21.6409 (1990).
125 Scientific, T. F. *Real-time PCR handbook*, <https://www.thermofisher.com/content/dam/LifeTech/global/Forms/PDF/real-time-pcr-handbook.pdf> (2014).
126 Wacker, M. J. & Godard, M. P. Analysis of one-step and two-step real-time RT-PCR using SuperScript III. *J Biomol Tech* **16**, 266-271 (2005).
127 QIAGEN®. *QIAzol® Handbook*, <https://www.google.com/url?sa=t&rct=j&q=&esrc=s&source=web&cd=&ved=2ahUKEwiPyoTl2MvwAhXm-SoKHW9NAhIQFjABegQIAxAD&url=https%3A%2F%2Fwww.qiagen.com%2Fus%2Fresource

s%2Fdownload.aspx%3Fid%3D6c452080-142a-44a7-a902-9177dea57d7c%26lang%3Den&usg=AOvVaw28GUKT1yh_36Zk2wmAdNmX> (2009).
128 RESEARCH, Z. *Direct-zol™ RNA Miniprep Plus*, <https://files.zymoresearch.com/protocols/_r2070t_r2070_r2071_r2072_r2073_direct-zol_rna_miniprep_plus_kit.pdf> (2021).
129 Quantabio. *PerfeCTa SYBR Green FastMix*, <https://www.quantabio.com/media/contenttype/IFU-050.1_REV_02_95073_PerfeCTa_SYBR_Green_FastMix_ROX.pdf> (2020).
130 Harber, K. J. *et al.* Succinate is an inflammation-induced immunoregulatory metabolite in macrophages. *Metabolites* **10**, 372 (2020).
131 Li, X., Mao, M., Zhang, Y., Yu, K. & Zhu, W. Succinate Modulates Intestinal Barrier Function and Inflammation Response in Pigs. *Biomolecules* **9**, doi:10.3390/biom9090486 (2019).
132 Ge, H., Zhao, S., Lü, X., Chuang, E. Y.-Y. & Ching, W.-M. Gene expression Profile of THP-1 cells infected by R. prowazekii suggests host response signature genes. *The Open Infectious Diseases Journal* **2** (2008).
133 Silver, N., Best, S., Jiang, J. & Thein, S. L. Selection of housekeeping genes for gene expression studies in human reticulocytes using real-time PCR. *BMC Mol Biol* **7**, 33, doi:10.1186/1471-2199-7-33 (2006).
134 Maess, M. B., Sendelbach, S. & Lorkowski, S. Selection of reliable reference genes during THP-1 monocyte differentiation into macrophages. *BMC Mol Biol* **11**, 90, doi:10.1186/1471-2199-11-90 (2010).
135 Zhang, H. *et al.* Comprehensive analysis of neuronal guidance cue expression regulation during monocyte-to-macrophage differentiation reveals post-transcriptional regulation of semaphorin7A by the RNA-binding protein quaking. *Innate immunity* **27**, 118-132 (2021).
136 Panina, Y., Germond, A., Masui, S. & Watanabe, T. M. Validation of Common Housekeeping Genes as Reference for qPCR Gene Expression Analysis During iPS Reprogramming Process. *Scientific Reports* **8**, 8716, doi:10.1038/s41598-018-26707-8 (2018).
137 Van Acker, S. I. *et al.* Selecting Appropriate Reference Genes for Quantitative Real-Time Polymerase Chain Reaction Studies in Isolated and Cultured Ocular Surface Epithelia. *Scientific Reports* **9**, 19631, doi:10.1038/s41598-019-56054-1 (2019).
138 Rothe, M., Wong, S. C., Henzel, W. J. & Goeddel, D. V. A novel family of putative signal transducers associated with the cytoplasmic domain of the 75 kDa tumor necrosis factor receptor. *Cell* **78**, 681-692, doi:10.1016/0092-8674(94)90532-0 (1994).
139 Huang, J., Gao, X., Li, S. & Cao, Z. Recruitment of IRAK to the interleukin 1 receptor complex requires interleukin 1 receptor accessory protein. *Proceedings of the National Academy of Sciences* **94**, 12829-12832 (1997).
140 Li, H., Xu, H. & Liu, S. Toll-like receptors 4 induces expression of matrix metalloproteinase-9 in human aortic smooth muscle cells. *Mol Biol Rep* **38**, 1419-1423, doi:10.1007/s11033-010-0246-4 (2011).
141 Li, H., Xu, H. & Sun, B. Lipopolysaccharide regulates MMP-9 expression through TLR4/NF-κB signaling in human arterial smooth muscle cells. *Molecular medicine reports* **6**, 774-778 (2012).
142 Chakraborty, S. *et al.* The use of nano-quercetin to arrest mitochondrial damage and MMP-9 upregulation during prevention of gastric inflammation induced by ethanol in rat. *Biomaterials* **33**, 2991-3001, doi:https://doi.org/10.1016/j.biomaterials.2011.12.037 (2012).
143 Kim, E.-Y. & Kim, B.-C. Lipopolysaccharide inhibits transforming growth factor-beta1-stimulated Smad6 expression by inducing phosphorylation of the linker region of Smad3 through a TLR4–IRAK1–ERK1/2 pathway. *FEBS Letters* **585**, 779-785, doi:https://doi.org/10.1016/j.febslet.2011.01.044 (2011).
144 Littlewood-Evans, A. *et al.* GPR91 senses extracellular succinate released from inflammatory macrophages and exacerbates rheumatoid arthritis. *J Exp Med* **213**, 1655-1662, doi:10.1084/jem.20160061 (2016).

# APPENDIX

**Supplementary table 1: Standard curve for protein concentration (microplate procedure).**

| Vial | Volume of diluent ($H_2O$) (µl) | Volume and source of BSA (µl) | Final BSA concentration (µg/ml) |
|---|---|---|---|
| A (Stock) | 0 | 300 | 2000 |
| B | 125 | 375 | 1500 |
| C | 325 | 325 | 1000 |
| D | 175 | 175 of vial B solution | 750 |
| E | 325 | 325 of vial C solution | 500 |
| F | 325 | 325 of vial E solution | 250 |
| G | 325 | 325 of vial F solution | 125 |
| H | 400 | 100 of vial G solution | 25 |
| I (Blank) | 400 | 0 | 0 |

**Supplementary table 2: Forward and reverse primer sequences of target genes.**

| Gene | Primer F | Primer R |
|---|---|---|
| *18S* | AACTTTCGATGGTAGTCGCCG | CCTTGGATGTGGTAGCCGTTT |
| *ACTB* | TCATGAAGTGTGACGTTGACATCCGT | CCTAGAAGCATTTGCGGTGCACGATG |
| *GAPDH* | CGAGATCCCTCCAAAATCAA | TTCACACCCATGACGAACAT |
| *TBP* | TTGCTGCGGTAATCATGAGG | GCCAGTCTGGACTGTTCTTC |
| *TNF-α* | ATGAGCACTGAAAGCATGATCC | GAGGGCTGATTAGAGAGAGGTC |
| *IL-1β* | CAGCTACGAATCTCCGACCAC | GGCAGGGAACCAGCATCTTC |
| *MMP9* | ATCCAGTTTGGTGTCGCGGAGC | GAAGGGGAAGACGCACAGCT |
| *TGF-β1* | TCGCCAGAGTGGTTATCTT | TAGTGAACCCGTTGATGTCC |

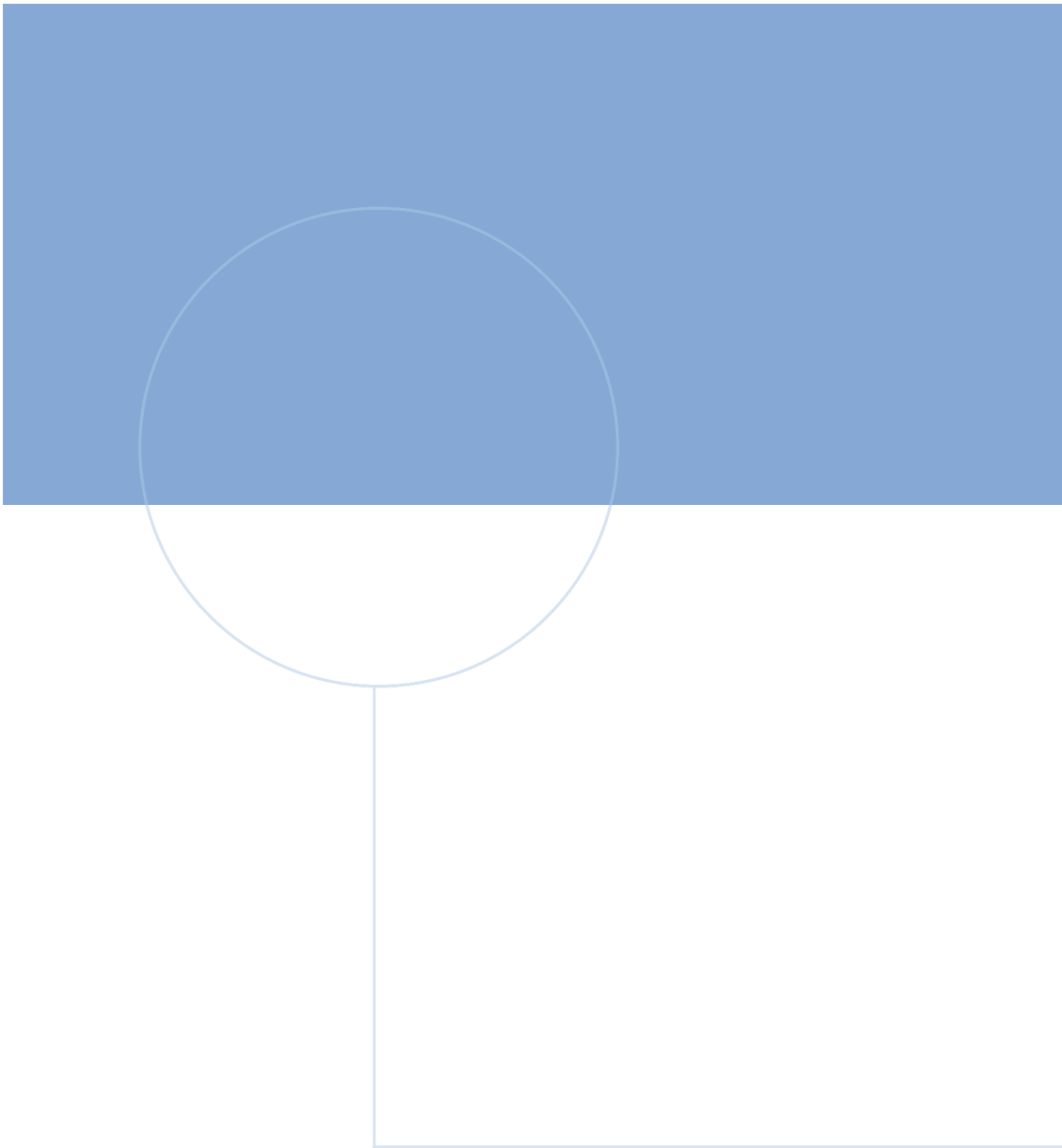

NTNU

Kunnskap for en bedre verden